To the Graduate Council:

I am submitting herewith a thesis written by John Blakemore entitled "*In vitro* phosphorylation of transcription factors ATF2 and ATFa." I have examined the final copy of this thesis for form and content and recommend that it be accepted in partial fulfillment of the requirements for the degree of Master of Science, with a major in Life Sciences.

Wesley D. Wicks, Major Professor

We have read this thesis and
recommend its acceptance:

Accepted for the Council:

Associate Vice Chancellor and
Dean of The Graduate School

In vitro phosphorylation of transcription factors ATF2 and ATFa.

A Thesis

Presented for the

Master of Science

Degree

The University of Tennessee, Knoxville

John L. Blakemore

August 1998

DEDICATION

This work is dedicated to my wife, Jennifer, who tolerated me through its construction, and to my Granny, who taught me that an education can never be taken from you.

ACKNOWLEDGEMENTS

I would like to thank my major professor, Dr. Wesley Wicks, for his boundless patience and his guidance in the writing of this thesis.

I am most grateful to my committee members, Dr. John Koontz and Dr. Tom Chen for their suggestions and their encouragement.

I would also like to thank my lab-mate, Huo Li, as well as all of the assistants that have worked in our lab, especially Mark Harman. Their advice and assistance is greatly appreciated.

Extra special thanks go to Rhonda Mattingly and the other secretaries who know how to get things done and kept me well stocked in transparencies and other necessities.

And finally, I would like to thank my wife, Jennifer, for her support and encouragement. I do it all for her.

ABSTRACT

ATF2 and ATFa are members of the bZip family of eukaryotic transcription factors, which are characterized by the presence of a region of basic amino acids (basic region) located upstream of a heptad repeat of leucine residues (leucine zipper). The leucine zipper region is required for dimer formation, and the basic region binds the negatively charged DNA backbone. ATF2 and ATFa are unique among the bZip transcription factors in that they both contain a metal binding domain (zinc finger) in their amino-terminus.

Both ATF2 and ATFa are able to bind DNA in a sequence specific manner, regulating transcription. This DNA binding requires the formation of homo- or heterodimers. These dimers bind DNA at sites called CREs, or cyclic AMP response elements (5'TGACGTCA3'), although neither transcription factor is able to confer cAMP responsiveness. Heterodimerization with the related transcription factor c-Jun enables binding to sites similar to CREs, called TREs (5'TGA C/G TCA3'), implying a method of fine tuning gene regulation. Genes shown to have ATF binding sites in their promoter region include TGF-β2, E-selectin, c-Jun, and TNFα.

Activation of transcription factors has been shown to be regulated through both protein-protein interactions and phosphorylation. Both ATF2 and ATFa are able to interact with the Hepatitis-B viral X protein, the Tax protein of human T cell leukemia, and the adenovirus E1a protein. Through direct interaction with E1a, both ATF2 and

ATFa are able to activate transcription through CRE sites. Phosphorylation of ATF2 on threonine residues 69 and 71 in response to environmental stress such as UV light, heat shock, hyperosmolarity, and alkylating agents has been shown to be a requirement for transcriptional activation. This phosphorylation is due to members of the JNK and p38 family of mitogen activated protein (MAP) kinases, and although other kinases have been reported to phosphorylate ATF2, none have been shown to mediate its activity. The direct effect of phosphorylation of ATF2 has not been elucidated, but possibilities include a conformational change that enables dimerization (and thereby DNA binding), disruption of intramolecular N-terminal/C-terminal inhibitory interactions, or facilitating protein-protein interactions either directly to the basal transcription machinery or to a bridging protein that in turn binds to the transcription machinery.

Because ATF2 has been the subject of more research than ATFa, and because of the many similarities between these proteins, I chose to focus on ATFa for my experiments. Two kinases were purified, one purchased, and all three were tested for their ability to phosphorylate both purified ATF2 and ATFa. The cyclic AMP-dependent protein kinase (PKA) was able to phosphorylate both transcription factors, as was JNK_1. A surprising difference was found when p38 was tested, however. While ATF2 proved to be a substrate for p38, ATFa was not able to be phosphorylated by this kinase under any conditions tested. Because the site of phosphorylation in ATF2 by p38 is highly conserved in ATFa, this proved to be a surprising and unique discovery.

Table of Contents

CHAPTER

1 Introduction..... 1

2 Materials and Methods..... 15

Cell cultures..... 15

Nickel Affinity Chromatography..... 15

Preparation and Purification of GST fusion proteins..... 16

JNK_1 and p38 kinase assays..... 17

PKA kinase assay..... 17

Western blotting..... 18

3 Results and Discussion..... 20

Purification of ATFa by nickel-sepharose affinity chromatography 20

Determination of the concentration of ATFa..... 21

Phosphorylation of ATF2 by GST-JNK_1..... 22

Phosphorylation of ATFa by GST-JNK_1..... 24

PKA phosphorylation of ATF2 and ATFa..... 25

GST-p38 phosphorylation of ATF2..... 26

Titration of ATF2 and ATFa against GST-p38..... 27

GST-p38/ATFa time course..... 28

Titration of GST-p38 and ATFa..... 29

Conclusions..... 29

4 Future Studies..... 34

List of References..... 36

Appendix..... 43

Vita..... 64

List of Figures

Figure 1: Sequence Comparison of ATF2 and ATFa..... 44

Figure 2: Nickel-Sepharose Affinity Column Purification of ATFa..... 45

Figure 3: Affinity Column Purification of ATFa with Urea Gradient Wash..... 46

Figure 4: Comparison of Concentrations of Purified ATF2 and ATFa..... 47

Figure 5: GST-JNK_1/ATF2 Phosphorylation Time Course..... 48

Figure 6: Titration of GST-JNK_1 and ATF2..... 49

Figure 7: Densitometric Measurement of the Titration of ATF2 with GST-JNK_1..... 50

Figure 8: Densitometric Measurement of the Titration of GST-JNK_1 with ATF2..... 51

Figure 9: GST-JNK_1/ATFa Phosphorylation Time Course..... 52

Figure 10: Titration of GST-JNK_1 and ATFa..... 53

Figure 11: cAMP Dependent Kinase (PKA) Phosphorylation of ATF2 and ATFa..... 54

Figure 12: GST-p38/ATF2 Phosphorylation Time Course..... 55

Figure 13: Titration of GST-p38 and ATF2..... 56

Figure 14: Densitometric Measurement of the Titration of GST-p38 with ATF2..... 57

Figure 15: Densitometric Measurement of the Titration of ATF2 with GST-p38..... 58

Figure 16: Titration of GST-p38 with ATF2 and ATFa..... 59

Figure 17: Densitometric Measurement of the Titration of ATF2 with GST-p38..... 60

Figure 18: GST-p38/ATFa Phosphorylation Time Course..... 61

Figure 19: Titration of GST-p38 and ATFa..... 62

Figure 20: Densitometric Measurement of the Titration of GST-p38 with ATFa..... 63

LIST OF ABBREVIATIONS

ATF2	Activating Transcription Factor-2
ATFa	Activating Transcription Factor-a
AP-1	Activating Protein complex 1
bZip	basic-Leucine-Zipper
cAMP	Cyclic Adenosine 3', 5'-Monophosphate
CAT	Chloramphenicol Acetyltransferase
CBP	CREB Binding Protein
CKII	Casein Kinase II
CRE	cAMP Response Element
CREB	cAMP Response Element Binding-protein
DTT	Dithiothreitol
E1A	Adenovirus Early region 1A oncoprotein
ERK	Extracellular-signal Regulated Kinase
GSH	Glutathione
GST	Glutathione-S-Transferase
HMG I (Y)	High Mobility Group protein I (Y)
INF-β	Human interferon β
JNK	cJun N-terminal Kinase

MBP	Myelin Basic Protein
MMNG	N-methyl-N'-nitro-N-nitroso-guanidine
MMS	Methylmethane Sulphonate
NF-κB	Nuclear Factor κB
NLS	Nuclear Localization Signal
PKA	cAMP-activated Protein Kinase A
PP2A	Protein Phosphatase 2A
pRB	Retinoblastoma Gene Product
PRD	Positive Regulatory Domain
SAPK	Stress-Activated Protein Kinase
TGF-β2	Human Transforming Growth Factor β2
TNFα	Tumor Necrosis Factor α
TRE	12-O-tetradecanoyl-phorbol-13-acetate Response Element

Chapter 1

Introduction

ATF2 is a 505 amino acid protein (54.5 kD) expressed in various human tissue types including lung, liver, kidney and it is especially abundant in the nervous system and brain cells such as hippocampus and dentate gyrus (Maekawa et al., 1989). The ATF2 gene is located on human chromosome 2 and this gene's promoter has no TATA box but does contain several Sp-1 binding sites (Goetz et al., 1996). A germline mutation of the ATF2 gene in mice caused a 49% mortality rate within a month of birth. Those mice surviving the first month thereafter had a mortality rate double that of normal mice. These survivors were runted, only achieving 71% of normal weight, with dwarfism of the spine and long bones as well as deafness and hyperactivity. The ATF2 (-/-) mice also had smaller brains, with a 50% decrease in the number of Purkinje cells. They also displayed body-wide twitching, head twitching, and decreased hind limb coordination (Reimold et al., 1996). These defects indicate ATF2 is required for skeletal system and nervous system development.

ATF2 is a bZip protein, with a highly conserved dimerization and DNA binding domain. ATF2 forms homodimers that bind to CRE sites and can form heterodimers with cJun. ATF2 fails to dimerize with JunB or cFos (Chatton et al., 1994). ATF2/cJun heterodimers can bind to CRE (5'TGACGTCA3') and 12-O-tetradecanoyl-phorbol-13-acetate response element (TRE) (5'TGAGTCA3') with high affinity, as well as the NF-ELAM element (5'TGACATCA3') (Hai and Curran, 1991).

ATF2 is able to mediate the transactivation ability of E1a *in vivo*. Using a GAL4-ATF2 fusion protein with a CAT reporter containing GAL4 binding sites in its promoter region, ATF2 has been shown to mediate transcriptional activation through the E1a oncogene product, while neither ATF2 nor E1a alone could activate transcription in this system. Deletion of amino acids 1-33 (the zinc finger domain) in ATF2 reduced E1a inducibility in this system by four fold. Further deletion to residue 108 reduced activity by 10 fold (Liu and Green, 1990). Mutation of Thr 69 or Thr 71 to alanine either individually or together in GAL4-ATF2 fusion proteins reduced E1a activation in CAT reporter constructs with GAL4 promoters by 5-fold. Mutation of Ser 90 to alanine mediated an E1a response as well as the wild-type ATF2 protein in this system. E1a and ATF2 can interact directly. This was demonstrated in an affinity pull-down experiment. GST-E1a immobilized on GSH-agarose beads was incubated with cell extracts overexpressing ATF2 truncation mutants. E1a was only able to interact with ATF2 mutants that included amino acids 350-505. Thus while the N-terminal region of ATF2 is required to mediate E1a transactivation ability, it is the C-terminal 155 amino acids that are required for protein-protein interaction (Livingstone et al., 1995).

ATF2 has three sites for phosphorylation by proline directed kinases in the amino-terminus. These sites are threonine 69 and 71 and serine 90. JNK_1 binds ATF2 directly through interactions requiring the N-terminus of ATF2 (between amino acids 20 and 60) and phosphorylates each of these sites. Full length ATF2 was not as good a substrate for this reaction as were N-terminal domain truncations, indicating that the kinase may have difficulty accessing the site of phosphorylation due to the conformation of the full length

ATF2 protein (Livingstone et al, 1995). Mutation of Thr 69, Thr 71 and Ser 90 to alanine abolished phosphorylation by JNK_1 *in vitro*. These sites are also phosphorylated by ERK2 *in vitro* but not as efficiently as with JNK_1. ATF2 has been shown to directly interact with JNK_1 by affinity pull-down experiments. Immobilized GST-ATF2 proteins incubated with extracts from UV-stimulated cells were able to bind JNK_1 and JNK_2, and mutation of any of the phosphoacceptor sites had no effect on this binding. Phosphopeptide mapping of wild-type and mutant ATF2 peptides indicated the phosphorylation of Thr 69, Thr 71 and Ser 90 *in vivo* (Livingstone et al., 1995).

In vivo studies with GAL4-ATF2 fusion proteins in F9 cells (which lack endogenous cJun or cFos) transfected with a CAT reporter containing GAL4 binding sites in the promoter region revealed that exposure to UV light activated transcription through ATF2/cJun heterodimers (van Dam et al., 1995). The cJun promoter elements *jun1* and *jun2* are constitutively occupied in the F9 cells, and activation was due to phosphorylation of ATF2/cJun heterodimers. Threonines 69 and 71 in ATF2 are required for this effect and a truncation mutation consisting of only amino acids 1-112 (including the activation domain) was sufficient to convey transcriptional activity (van Dam et al., 1995). Treatment with TPA did not activate ATF2, but it did activate cJun, indicating that ATF2 is not a target of the ERK cascade induced by phorbol esters *in vivo*. The alkylating agents MNNG (N-methyl-N'-nitro-N-nitroso-guanidine) and MMS (methylmethane sulphonate), which damage DNA, increased transcription of a GAL-4 promoter through ATF2 by 5-fold, and Thr 69 and Thr 71 are required, while Ser 90 is not (van Dam et al., 1995), further defining conditions under which ATF2 is activated.

The ATF2 C-terminal domain (including the bZip region) between amino acids 349 and 415 has been shown to be able to bind to the N-terminal domain of ATF2 and inhibit transcriptional activation (Liu and Green, 1996). Neither the basic region nor the leucine zipper alone supports this interaction; instead both are required. The bZip domain from cFos fused to amino acids 1-349 of ATF2 did not confer this inhibition, but the bZip domains of CREB, CEBP and cJun did. Immobilized GST-ATF2 1-109 or GST-ATF2 1-139 were able to bind bacterially expressed full length ATF2, implying this interaction is specific. Fusing the bZip and zinc finger domains together in various combinations shows that this inhibition is independent of the relative position of these two domains within the same molecule (Liu and Green, 1996). This inhibition may be a mechanism to prevent transcription factors from binding to DNA under non-activating conditions.

ATF2 may activate transcription by recruitment of the basal transcription machinery, perhaps through protein-protein interactions with the N-terminal domain of the transcription factor. One model of how this may occur involves HMG I(Y) and NF-κB proteins in the INF-β promoter (Du et al., 1993). HMG I(Y) is able to bind DNA and recruit NF-κB to PRD promoter sites. Two of these sites in the IFN-β promoter flank ATF/CRE sites. Two HMG I(Y) proteins bind to these PRD sites and recruit ATF2/cJun heterodimers to the IFN-β promoter (Du et al., 1993), perhaps overriding the need for phosphorylation to enable dimerization or DNA binding. A CAT reporter system with an IFN-β promoter in HeLa cells was used to test the effect of antisense RNA expressing vectors for ATF2, NF-κB or HMG I(Y). These experiments showed the need for all three proteins in induction of transcription in this system. Antisense cJun reduced reporter

activity, but not to a similar level as did antisense ATF2, implying that ATF2 homodimers as well as ATF2/cJun heterodimers play a role in this activation. HMG I(Y) binds both ATF2 and cJun, and this interaction requires the bZip domain. This interaction serves to recruit ATF2/cJun heterodimers to the ATF/CRE site in the IFN-β promoter. HMG I(Y) binds DNA in the minor groove, allowing the binding site to overlap that of ATF2. This binding may cause the DNA to bend and allow the assembly of the transcription complex (Du et al, 1993). This complex involves a pair of HMG I(Y) proteins bound simultaneously to DNA and ATF2 dimers, which in turn is bound to NF-κB, itself bound to a pair of HMG I(Y) proteins. Both ATF2 and NF-κB interact with the basal transcription machinery in this model, giving the most complete model for the possible mechanism of ATF2 function to date.

The transcription factor most closely related to ATF2 is ATFa. The two factors share many similarities, but significant differences in function have been observed (Gong et al., 1995). ATFa is a 483 amino acid protein with a projected molecular weight of 51.7 kD. The gene for human ATFa is found on chromosome 12, and ATFa mRNA transcripts were found at low levels in human cell lines such as HeLa, JEG-3, MCF 7, 293 cells and MG 63 (Goetz et al., 1996). The ratio of ATFa mRNA transcripts as compared to ATF2 and CREB is 1:5:20 (Goetz et al., 1996). ATFa is expressed in mouse embryos and most adult mouse organs, and elevated levels were detected in squamous or pseudostratified epithelia, as well as in specific areas of the brain such as Purkinje cells, the hippocampus, dentate gyrus, and piriform cortex (Goetz et al., 1996). The promoter region of the ATFa

gene has neither a TATA box nor an ATF/CRE site, being more similar to the ATF2 promoter than to other ATF genes (Goetz et al., 1996).

There are 4 splice variants of ATFa currently known. One forms a dominant inhibitor with ATFa, completely blocking ATFa's transactivating ability (Pescini et al., 1994). This variant, known as ATFa0, is missing 176 amino acids (135-310). One variant, ATFa3, has an extra 11 amino acids, while another, ATFa1, is missing 21 amino acids between positions 125-145 (Chatton et al., 1993). All three full length variants, ATFa1, ATFa2 (commonly known as simply ATFa) and ATFa3, are able to mediate E1a induction of a CAT reporter construct in HeLa cells. All three were also able to be co-precipitated with antibodies to cFos and cJun, and antibodies to ATFa were able to isolate both cJun and cFos(Chatton, et al., 1993). GAL4-ATFa/cJun heterodimers with all three variants were able to stimulate a GAL4 reporter construct up to 13 fold (Chatton, et al., 1994).

Like the other members of the bZip family of transcription factors, ATFa has a highly conserved region containing a leucine zipper motif that is responsible for dimerization C-terminal from a region of basic amino acids (Meyer and Habener, 1993). This basic region is the site responsible for DNA binding, conferring specificity to the dimer. ATF homodimers bind to a site inside the CRE called the ATF site (5'TGACGTCA3'). This site differs from the related TRE site (5'TGAGTCA3') bound by related transcription factors cJun/cFos heterodimers by a single nucleotide (5'TGAGTCA3').

Like ATF2, ATFa is different from other bZip transcription factors in that both have a zinc binding element in the N-terminus. This region has been shown to be

responsible for E1a responsiveness (but not E1a binding). The N-terminal 88 amino acids are involved in JNK_2 binding (Bocco et al., 1996). A point mutation (His27 to Asn) in the zinc finger domain destroys this effect on E1a activity (Chatton et al., 1993). This region is also able to bind to and mask the C-terminal end of ATFa, between amino acids 378 and 456 (Goetz et al., 1996). It is believed that this interaction masks the DNA binding and dimerization domain as a form of negative regulation (Goetz et al., 1996). Deletion of this region in GAL4 fusion proteins resulted in nearly maximal CAT reporter activity (Chatton, et al., 1994b). Phosphorylation may cause a conformational change that disrupts this negative regulation and enable dimerization and DNA binding.

ATFa has been shown to dimerize with cJun and cFos. ATFa/cJun heterodimers can bind both CREs and TREs, as well as AP1 sites, while ATFa/cFos heterodimers cannot bind either (Chatton, et al., 1994b). Co-expression of cJun and GAL4-ATFa plasmids resulted in up to 13 fold increases of transcription of a GAL4-TK-CAT reporter (Chatton, et al., 1994b). This activation was not dependent on the transactivation domain of ATFa, since deletion of amino acids up to 278 had no effect on the observed stimulation. Deletion of the bZip region destroyed cJun-mediated activation. Similar results were seen with ATFa/JunD and ATFa/JunB heterodimers. The interaction between ATFa and cJun was also observed *in vivo* by immunoprecipitation experiments in cultured COS-7 cells. Deletion of the bZip domain greatly reduced the amount of cJun coprecipitated with anti-ATFa antibodies (Chatton, 1994). The C-terminus also contains a nuclear localization signal (NLS) between amino acids 327-368. Immunofluorescent staining experiments with ATFa antibodies show nuclear localization in HeLa cells

overexpressing ATFa (Goetz et al., 1996). An unidentified kinase was co-immunoprecipitated using a GST fusion protein linked to the basic region of ATFa's bZip domain (Bocco et al, 1996). The level of phosphorylation of ATFa by this kinase was less than that observed with JNK_2. This kinase is not stimulated by ultraviolet light nor heat-shock, as is the case with JNKs, but was slightly responsive to TPA, like the ERKs. The effect of either of these kinases on ATFa activity has yet to be determined.

Like ATF2, ATFa has been shown to interact directly with NF-κB (Kaszubska et al., 1993). In the E-selectin promoter, ATFa and ATF2 homodimers, as well as ATF2-cJun heterodimers bind to the NF-ELAM1 site, which contain a CRE-like sequence (5'TGACATCA3'). In an E-selectin CAT reporter, overexpressed ATFa was able to activate transcription, whereas ATF2 could not (Kaszubska et al., 1993). In an affinity pull-down experiment, both ATFa and ATF2 were able to directly interact with subunits of NF-κB. GST fusion proteins of p50 and p65 NF-κB were able to bind to ATFa and ATF2, and this interaction was estimated to require the bZip region of the ATFs. An ATF2 clone missing amino acids 1-107 (including the zinc finger and JNK/p38 phosphorylation sites) and ATFa0 (missing amino acids 135-310) were able to interact with the p50 subunit of NF-κB. Both of these ATF variants contain the bZip domain, indicating this is the region responsible for NF-κB binding (Kaszubska et al., 1993). While ATFa was not shown to bind the basal transcription machinery in this model, it is reasonable to theorize activation similar to that in the ATF2/NF-κB/HMG I(Y) model of the INF-β promoter (Du et al., 1993). Note that this may be a unique model, and other ATF-containing transcription initiation complexes may differ considerably.

ATFa and ATF2, like other transcription factors, can have their actions regulated in several ways, the most studied being phosphorylation. There are at least three distinct kinase cascades in mammalian cells, with evidence of some cross-talk reported. These cascades are the extracellular signal-related kinase (ERK) pathway, the stress activated protein kinase (SAPK) or c-Jun N-terminal kinase (JNK) pathway, and the p38 pathway. MAP kinases p42 (ERK1) and p54 (ERK2) have been shown to phosphorylate ATF2 *in vitro*, and this phosphorylation had the effect of enabling bacterially expressed ATF2 to become competent to bind DNA (Abdel-Hafiz et al., 1992). The catalytic subunit of the cAMP dependent kinase (PKA) has also been shown to phosphorylate ATF2, but no effect on DNA binding was evident (Abdel-Hafiz et al., 1992). This observation is consistent with the lack of cAMP responsiveness displayed by both ATF2 and ATFa (Meyer and Habener, 1993). Dephosphorylation by protein phosphatase 2A (PP2A) of ATF2 previously phosphorylated by ERK1/2 reversed its ability to bind DNA in gel shift assays, indicating a role of phosphorylation in regulation of DNA binding (Abdel-Hafiz et al., 1992). However, more recent studies indicate the JNK isoforms and p38 may have more physiologically relevant roles. JNK_1 has been shown to phosphorylate ATF2 on threonine residues 69 and 71, and to a lesser extent, serine 90 (Livingstone et al., 1995). Mutation of these sites to alanine individually or in combination in GAL4 fusion proteins destroyed the ability of ATF2 to enhance a CAT reporter's transcriptional activity with a GAL-4 promoter (Livingstone et al., 1995). These same mutations also decreased E1a activation in a similar reporter construct (Liu and Green, 1990). Since the N-terminal domain in ATF2 is highly conserved in ATFa, including the crucial threonine residues (at 51 and 53

in ATFa), it is likely that one or more of the kinases able to phosphorylate ATF2 may also be able to phosphorylate ATFa. Indeed, ATFa has been shown to bind JNK2 directly and is a substrate for that kinase (Bocco et al., 1996).

UV light, TNF-α, heat shock, anisomycin, hyperosmolarity and arsenite not only activate the JNK pathway *in vivo*, but also the p38 pathway. Simultaneous activation of JNK and p38 along with the inactivation of the ERK pathway lead to an increase in the number of apoptotic rat PC-12 pheochromocytoma cells (Xia et al., 1995). ATF2 has been shown to be a substrate for p38, and the sites of this phosphorylation are the same as seen with JNK, namely threonines 69 and 71 (Raingeaud, et al., 1995, and Raingeaud, et al., 1996). Studies have also shown that p38 phosphorylates ATF2 while ATF2 is bound to DNA in the E-selectin promoter. This suggests that phosphorylation of ATF2 by p38 does not lead to dimerization or DNA binding, instead this phosphorylation may lead to activation by recruiting basal transcription machinery such as CBP or p300 (Read et al., 1997). Phosphorylation by other kinases may be a prerequisite to DNA binding, but not by p38. Variants of p38 have been discovered that phosphorylate ATF2 much better than has been seen with p38. The variants p38-2 and p38β2 phosphorylated ATF2 with a catalytic activity of over 100 fold more than p38 (Stein et al., 1997, and Kumar et al., 1997). Another variant, p38γ, was able to phosphorylate the known p38 substrate MBP, but surprisingly, not ATF2. This kinase is predominantly expressed in skeletal muscle, as opposed to the wider distribution of other forms of p38, implying a more cell-type specific role for this kinase (Li et al., 1996).

ATF2 as well as ATFa are able to influence the transcriptional activity of a TGF-β2 promoter-driven CAT reporter *in vivo* (Gong et al., 1995). Cotransfection of CHO cells with an ATFa expressing vector resulted in activation of the TGF-β2 driven CAT reporter. The same results were found with ATF2. Addition of cAMP had no effect on this activity, indicating that while both ATF2 and ATFa bind CREs, neither seem to be part of the cAMP signaling pathway. When ATF2 is overexpressed in this system along with pRb, transcription is greatly (more than additively) enhanced. Conversely, when pRb is coexpressed with ATFa, transcription is inhibited. Despite the many similarities between ATF2 and ATFa, there is obviously some difference in their functionality. Differing effects on transcription by ATF2 and ATFa may be mediated by levels of expression of the factors themselves. The ratio of mRNA levels of ATFa, ATF2, and CREB detected in HeLa cells was 1:5:20 (Goetz et al., 1996). Another means of regulation could involve alternately spliced variants, ATFa0 and mXBP2, that preferentially form inactive heterodimers with ATFa and ATF2, respectively (Pescini et al., 1994). Evidence has been shown in both proteins that the bZip domain binds to the activation domain, causing inhibition of dimerization and therefore DNA binding ability. Phosphorylation has been implicated as the means of reversing this intramolecular interaction, as well as induction of the N-terminal domain activation of transcription.

In summary, ATFa and ATF2 are two closely related members of the b-Zip family of transcription factors. Both have been shown to bind CREs very strongly *in vitro* (Maekawa et al., 1989, Gaire et al., 1990, Kim et al., 1992, and Liu and Green, 1990), although neither are able to confer cAMP responsiveness *in vivo* (Liu and Green, 1990).

The sequence similarity between the proteins include an 80% identity in the b-Zip region and a 86% identical sequence in an 88 amino acid N-terminal sequence (Gaire et al., 1990). Alignment of the sequences of these two transcription factors, as seen in Figure 1[1] suggests that ATFa and ATF2 are products of gene duplication, and have subsequently diverged through evolution (Meyer and Habener, 1993). Both have been shown to mediate the transcriptional activation ability of the adenovirus E1a protein (Chatton et al., 1993, and Liu and Green, 1990).

Both ATFa and ATF2 heterodimerize with cJun and these dimers are able to bind CREs (TGACGTCA) and TREs (Meyer and Habener, 1993, and Pescini et al., 1994). ATFa can also heterodimerize with cFos, whereas ATF2 cannot (Hai and Curran, 1991, and Chatton, 1994). ATFa/cFos heterodimers do not appear to bind either CRE nor TRE sites (Chatton, 1994). Both ATFa and ATF2 are able to bind CREs as homodimers. ATFa but not ATF2 has been shown to interact with Jun-B and Jun-D (Chatton, 1994). This dimerization ability is due to the leucine zipper region of the b-Zip domain. A leucine residue is repeated every seven amino acids in an alpha-helical section of the C-terminus. This arrangement places a series of 5 hydrophobic leucines on the same side of the alpha-helical region. Hydrophobic interactions with other leucine zippers enables dimerization. In ATFa this region runs from 359-387, and in ATF2 the region is between 380-408. There are only four amino acids that differ between ATFa and ATF2 in this region (an 86% identity). The other half of the b-Zip domain is the region of predominantly basic amino acids just N-terminal to the leucine zipper region. The positively charged amino

[1]All figures may be found in the Appendix on page 43.

acids of this basic region interact directly with the major groove of the negatively charged DNA backbone, providing DNA specificity for the transcription factors (Meyer and Habener, 1993). There are only two amino acids different between ATFa and ATF2 in this region.

The N-terminal domains of ATFa and ATF2 differ from other related transcription factors in that they have a zinc binding region. Deletion of this region (1-143) in ATF2 results in the destruction of E1a inducibility (Liu and Green, 1990), as well as destroying activation of TGF-β2 (Kim et al., 1992). Deletion of amino acids 1-33 in ATFa also abolished E1a responsiveness in a GAL4 fusion protein system (Chatton, 1993). The N-terminal domain in both proteins has been shown to be a binding site for protein-protein interactions and also necessary for transactivation ability.

Despite the many similarities between ATF2 and ATFa, little attention has been paid to the ability of ATFa to serve as a substrate for kinases known to phosphorylate ATF2. ATF2 has been shown to be phosphorylated by PKA, JNK, and p38 in several studies (Abdel-Hafiz et al., 1992, Livingstone et al., van Dam et al., 1995, Gupta et al., 1995, Raingeaud, 1995, Raingeaud, 1996, and Read et al., 1997), but only one paper has investigated the phosphorylation of ATFa (Bocco et al., 1996). ATFa was able to bind to a kinase identified as JNK_2 through immunoprecipitation experiments in HeLa and COS-7 cells. A fusion protein consisting of GST and the 82 N-terminal amino acids of ATFa was able to trap JNK_2 from crude cellular lysates. Another kinase was able to interact with the carboxyl terminal end of ATFa, but the identity of this kinase was never determined

(Bocco et al., 1996). Thus, I decided to compare the ability of various kinases to phosphorylate both ATF2 and ATFa *in vitro*, including JNK_1, PKA, and p38.

Phosphorylation of ATF2 and ATFa by GST-JNK_1 and PKA proceeded as expected, with both transcription factors proving to be substrates for both kinases. But an unexpected difference was found when ATFa and ATF2 were used in assays with the kinase p38. GST-p38 phosphorylated ATF2, as was reported previously; however, ATFa was not phosphorylated by GST-p38 under any experimental parameters tested. This is a unique discovery, due to the fact that the phosphoacceptor sites for p38 in ATF2 are highly conserved in ATFa, as well as the upstream and downstream regions. The difference in substrate affinity may be due to the *in vitro* nature of the kinase assays used, but recent findings by Liu and Wicks (unpublished results) discount this option. Overexpression of MKK6 (a potent upstream activator of p38 but not JNK) and ATF2 in CHO cells resulted in activation of a CAT reporter with a TGFβ2 promoter, but overexpression of MKK6 with ATFa in the same system did not. Overexpression of MKK7, a potent activator of the JNK but not the p38 pathway, along with either ATFa or ATF2 resulted in increased CAT reporter activity. These results, taken with my *in vitro* results indicate that ATFa is a target of the JNK pathway, but not the p38 kinase pathway.

Chapter 2

Materials and Methods

Cell Cultures

Colonies of BL21 (DE3) pLysS *Escherichia coli* cells previously transformed with a vector expressing ATF-a (pET-14b), p38 or JNK_1 (pGEX) (Novagen) were taken from LB-Amp plates and incubated overnight in 30 ml of LB media containing 20 μg/ml of ampicillin at 37° with shaking. This culture was transferred to larger flasks with LB-Amp (1000 ml total volume) and incubated for 2 hours at 37° with shaking before being induced with IPTG (Sigma) at a final concentration of 0.4 mM. The incubation was carried on for 3 more hours before harvesting by centrifugation for 10 minutes at 5,000x g. Crude lysates were made by resuspending the pellets in 1x binding buffer (20 mM Tris pH 7.9, 500 mM NaCl, 5 mM imidazole (Sigma)) with 1 mM PMSF (Sigma), 0.3 μg/ml pepstatin A and 0.1 μg/ml leupeptin (the last two were a gift from the lab of Dr. Roberts) and then sonicating the cells on ice. Cellular debris was removed through centrifugation for 5 minutes at 10,000x g. Negative controls (untransformed cells and cells transformed with an empty vector but without IPTG induction) were also prepared.

Nickel Affinity Chromatography

The 6xHis-tag is a repeat of six histidine residues added in frame to proteins expressed through the pET 14b vector system. Two similar methods were used to purify

the 6x His tagged proteins, ATFa and ATF2. Crude cellular lysates were passed over a 2.5 ml bed volume nickel affinity (NTA-sepharose, Novagen) column equilibrated with 1x binding buffer. In one experiment the sample was washed with an increasing gradient of imidazole in 1x binding buffer ranging from 5 mM to 100 mM. Target proteins were eluted with addition of 200 mM imidazole in binding buffer. In another experiment, the crude lysate was added as described previously. The column was then washed with a decreasing gradient of urea ranging from 6M to 0M. Samples were eluted with 40 mM then 200 mM imidazole in 1x binding buffer. One ml fractions were collected and examined on a silver stained SDS-PAGE.

Preparation and Purification of GST fusion proteins

Cultures of *E. coli* expressing a GST fusion protein (JNK_1 and p38) were grown and harvested as described above, except the pellets were resuspended in phosphate buffered saline (PBS) containing 1 mM DTT, 1 mM EDTA and 1 mM PMSF (each from Sigma). After sonication on ice, 10% Triton X-100 (Sigma) was added to the sample to a final concentration of 1%. Cellular debris was removed by centrifugation as above, with the supernatant being aliquoted as crude cellular lysate.

One ml of a 50% (v/v) slurry of GSH-agarose beads (Sigma) was then added to the crude lysate and incubated at room temperature for less than 5 minutes. Beads were collected by centrifugation in a table top centrifuge at 4° and washed 3 times with ice cold PBS-1 mM DTT/EDTA/PMSF. This pellet was resuspended in PBS-1 mM DTT/EDTA/PMSF and transferred to a 1.5 ml microcentrifuge tube. This volume of

buffer was discarded after another centrifugation at room temperature. GST tagged proteins were eluted off the GSH-agarose beads by the addition of elution buffer (50 mM Tris pH 8.0, 20 mM DTT, 10 mM reduced GSH) and incubation at room temperature for less than 5 minutes. Centrifugation at room temperature removed the GSH-agarose beads from the eluted fraction, which was saved. Sterile glycerol was added to the eluted fraction to a final concentration of 50% and the sample was stored at -20°.

JNK_1 and p38 Kinase Assays

Protein kinase GST-JNK_1 or GST-p38 (100 ng) were incubated with 5 μCi of ^{32}P-γ- ATP (ICN), 20 μM ATP (final), 20 μl assay buffer (25 mM HEPES, 25 mM $MgCl_2$, 25 mM β-glycerophosphate (Sigma), 1 mM DTT (Sigma), 0.1 mM sodium orthovanadate (Sigma)), substrate (typically 0.1 μg to 5 μg) and water to a final volume of 30 μl. This mixture was allowed to incubate at 30° for 30 minutes. The reaction was halted by addition of 5 μl of 5x Laemmli sample buffer (62.5 mM Tris, pH 6.8, 10% glycerol, 0.02% w/v SDS (Sigma), 0.02% w/v bromophenol blue (Sigma), 715 mM β-Mercapto-ethanol (Sigma)) and incubation at 95° for 5 minutes. Samples were then subjected to SDS-PAGE and the gels were washed twice in 1 M H_3PO_4 to reduce background. The gels were then Coomassie stained, destained, dried and exposed to x-ray film at -70° overnight with enhancing screen.

PKA Kinase Assay

The catalytic subunit of the cAMP dependent protein kinase (PKA) (Sigma) was resuspended in PKA resuspension buffer (300 mM KH_2PO_4, pH 6.8, 1 mM EDTA, 15 mM β-Mercapto-ethanol) to a final concentration of 2.5 units per µl. One µl of PKA was incubated with 20 µl PKA reaction buffer (25 mM MES pH 6.8, 5 mM $MgCl_2$, and 4 mM β-mercaptoethanol), 5 µCi ^{32}P-γ-ATP, 20 µM ATP (final), 0.1 µg to 5 µg substrate, and water to a final volume of 30 µl. The incubation was for 30° for 15 minutes. The reaction was terminated by addition of 5 µl of 5x Laemmli sample buffer and incubated at 95° for 5 minutes. After SDS-PAGE, the gels were washed twice in 1 M H_3PO_4 to reduce background, Coomassie stained, destained, dried and exposed to x-ray film at -70° overnight with enhancing screen.

Western Blotting

After resolving samples on a 10% SDS-PAGE and electroblotting onto nitrocellulose (Bio-Rad), 10% non-fat dry milk in PBS-0.05% Tween-20 (Mallinckrodt) ("blotto") was used to block non-specific proteins from binding to the membrane. After washing with PBS-Tween three times for 10 minutes, the primary antibody was added. This antibody was either monoclonal rabbit anti-ATF-2 (Santa Cruz), or monoclonal mouse anti-T7 (Novagen) in a final dilution of 1:3000. The T7 tag is an 11 amino acid leader peptide (Met-Ala-Ser-Met-Thr-Gly-Gly-Gln-Gln-Met-Gly) expressed by many pET expression vectors. After incubation with primary antibody, the membrane was washed with PBS-Tween before the secondary antibody was added (1:1000). The secondary antibodies were goat anti-mouse or goat anti-rabbit linked to horseradish peroxidase.

Bands were visualized by addition of 4-Chloro-1-naphthol (3mg/ml in methanol) and hydrogen peroxide (2µl/3ml) in PBS with shaking at room temperature.

Chapter 3

Results and Discussion

Purification of ATFa by nickel-sepharose affinity chromatography

6xHis-tagged ATFa was expressed in BL21(DE3) pLysS *E. coli* cells and crude cellular lysates were prepared as described in Materials and Methods. The polyhistidine tag binds nickel ions with high affinity, enabling rapid purification using nickel bound to sepharose. The crude lysate was loaded onto a 2 ml, pre-equilibrated, nickel-sepharose affinity column as described in Materials and Methods. The column was subsequently washed with a gradient of imidazole ranging from 5 to 100 mM. The His-tagged ATFa was eluted by the addition of 200 mM imidazole. Figure 2 shows the high degree of purification of ATFa achieved by this technique. In an attempt to remove the impurities seen with this procedure, another protocol was employed.

ATFa-containing crude cellular lysate was applied to a nickel affinity column as before, however, instead of washing with imidazole, the column was washed with a decreasing gradient of urea, ranging from 6 M to 0M. The urea wash causes denaturation of proteins bound to the affinity column, eliminating hydrophobic interactions that result in impurities co-eluting with his-tagged proteins. After the denaturing wash, the column was then washed with 40 mM imidazole and finally eluted with 200 mM imidazole. Figure 3A shows that a much higher degree of purity is achieved through this technique than that of the imidazole wash alone. The identity of the bands seen in the silver stained

polyacrylamide gel was confirmed through Western blotting, Figure 2B. The primary antibody used in this blot, mouse monoclonal anti-T7, is a highly specific antibody crafted against the 11 amino acid leader peptide expressed by the pET vector. This tag is fused in frame along with the His-tag and the ATFa cDNA and can therefore be used as an epitope tag specific to any protein expressed through the pET system, including ATF2 (see below). Figure 3B shows that both of the bands in the doublet seen in Figure 2 (lane 10) and Figure 3A (lanes 6 and 7) contain the T7 tag. Given the presence of the tag and the molecular weight of the doublet (69-71 kDa), both must be ATFa. The bands are either due to alternately spliced transcripts or, more likely, to proteolytic cleavage of the full length protein. Other researchers have also noticed that the mobility of the ATF proteins is lower in polyacrylamide gels than was expected given their projected weights. Using this technique, a much higher concentration of ATFa was purified, and to a much higher extent, apparently over 90% pure.

Determination of the concentration of ATFa

Known amounts of purified ATF2 (Santa Cruz) were resolved on a 10% polyacrylamide gel along with an unknown concentration of purified ATFa in an effort to approximate the concentration of ATFa. Figure 4A shows this silver stained gel. ATFa has 22 fewer amino acids than ATF2 (483 in ATFa, 505 in ATF2), and thus has a projected molecular weight 2.5-3.0 kDa less than ATF2 (51.7 as compared to 53.5 for the wild type proteins, plus 17 additional amino acids for the His and T7 tags). Both proteins were expressed in the same system and purified through similar techniques, resulting in some

similar impurities, but my preparation of ATFa appears to be cleaner than commercial ATF2. The ATFa band appears to be more intense than that of ATF2 seen in lane 2 (200 ng) but not as intense as the ATF2 band seen in lane 3 (400 ng). This implies that the concentration of ATFa is between 50 and 75 ng per µl. Notice also the breakdown product seen in the ATF2 lanes at a molecular weight of approximately 53 kDa. This product is also seen in the Western blot, Figure 4B, indicating that it must be an intact N-terminus. The estimated size of this breakdown product is estimated to be ~350 amino acids, based on its mobility in the SDS gel. This would correspond to cleavage of the bZip domain. The purified ATFa sample appears to be at least 90% pure, and while it is not as concentrated as the commercial ATF2, it is cleaner.

Phosphorylation of ATF2 by GST-JNK$_1$

It has been previously reported that ATF2 is a substrate for members of the JNK family of protein kinases (2-9, 2-10, 2-12). I tested the ability of my preparation of GST-JNK$_1$ to phosphorylate ATF2. GST-JNK$_1$ was purified as described in Materials and Methods. Approximately 50 ng of GST-JNK$_1$ was incubated with either GST-cJun (1-79), as a positive control, or 400 ng of ATF2 (Santa Cruz). Figure 5 shows an autoradiogram of a time course of ATF2 phosphorylation by GST-JNK$_1$ and the gel used to create the autoradiogram. The GST-JNK1 prepared in our lab is able to phosphorylate ATF2 (Santa Cruz). The 53 kDa ATF2 N-terminal breakdown product is also phosphorylated under these conditions. In fact, this breakdown product appears to be a better substrate than full length ATF2. There is much less of the breakdown product evident in the stained

polyacrylamide gel, but the band in the autoradiogram is intense. It appears that maximal phosphorylation of ATF2 occurs within 15 minutes of the initiation of the reaction. This may due to accidental loading of more sample in that particular well (Figure 5B, lane 5) than the actual rate of kinase activity.

Most of the GST-JNK_1 and GST-p38 kinase preparations exhibit a high degree of autophosphorylation (when the kinase phosphorylates itself at the activation sites normally phosphorylated by upstream kinases) and, unfortunately, the GST tag gives both kinases mobilities on SDS gels very similar to that of ATF2 and ATFa. This is problematic, but not impossible to work with, as long as the autophosphorylation band is not so intense as to overshadow that of ATF2 or ATFa. In assays with either kinase, ATF2 migrates above and ATFa below the kinase. Methods of correcting this problem include thrombin cleavage of the GST-tag or using GSH-agarose beads to remove the kinase. Nickel-sepharose beads can be used to isolate ATFa and ATF2. Attempts were made at using affinity beads to isolate either the kinase or the substrate, but various problems kept them from being as useful as first hoped. Densitometry, however, allows efficient differentiation between the bands. Upon scanning an autoradiogram with a densitometer, distinct peaks can be seen in adjacent bands as close as 0.1 mm apart.

Figure 6 shows the result of using increasing amounts of GST-JNK_1 with ATF2 and vice versa. Again, GST-JNK_1 shows a high degree of autophosphorylation, obscuring the visual detection of the GST-JNK_1 and ATF2 bands. Densitometry was able to distinguish between the two bands, however. Figure 7 shows that as the ATF2 concentration rises, the level of ATF2 phosphorylation rises, as does the level of the

breakdown product, roughly in proportion, as is expected. Figure 8 shows the relationship between increasing amounts of GST-JNK_1 and the degree of phosphorylation of full length ATF2 and the 53 kDa breakdown product. The degree of phosphorylation of the 53 kDa breakdown product is similar to that of the full length protein. The presence of the breakdown product is fortuitous, in a way, in that it mirrors the degree of phosphorylation of full length ATF2. This can serve as a guideline to the state of ATF2 phosphorylation when the full length protein band may be obscured by kinase autophosphorylation, without resorting to densitometry. From all of these results, I conclude that, as reported previously (Livingstone et al., 1995, van Dam et al., 1995, Gupta et al., 1995), ATF2 is a substrate for GST-JNK_1 *in vitro*. This phosphorylation of ATF2 serves as a control to compare phosphorylation of ATFa with GST-JNK_1, as examined below.

Phosphorylation of ATFa by GST-JNK_1

ATFa has been shown to bind JNK_2 directly and is phosphorylated by it *in vitro* (Bocco et al., 1996). To see if GST-JNK_1 could also phosphorylate ATFa, a GST-JNK1/ATFa time course assay was performed. Approximately 50 ng of GST-JNK_1 was incubated with either cJun (1-79) as a positive control or with approximately 300 ng of ATFa for up to 30 minutes in a time course assay, as done previously with ATF2. ATFa is efficiently phosphorylated by GST-JNK1 within 30 minutes (Figure 9). This particular preparation of GST-JNK_1 does not exhibit autophosphorylation, thus the phosphorylated band seen is clearly due to ATFa. Indeed, when the autoradiogram is overlaid onto the gel

that exposed the film, the bands superimpose directly over the ATFa bands (data not shown).

Figure 10 shows the results of varying the levels of GST-JNK_1 and ATFa relative to each other. As either concentration increases, the degree of ATFa phosphorylation also increases, although the effect of GST-JNK_1 concentration is more readily apparent. In lanes 7-9, the 50 ng of kinase may be quickly saturated with ATFa. Thus Figures 9 and 10 show ATFa is a substrate for GST-JNK_1 *in vitro*, just as is ATF2. In both cases, GST-JNK_1 efficient phosphorylation occurs in less than 30 minutes, and as little as 50 ng of kinase is sufficient to observe this activity.

PKA phosphorylation of ATF2 and ATFa.

It has been previously reported that the catalytic subunit of cAMP dependent kinase (PKA) can phosphorylate ATF2 (Abdel-Hafiz et al., 1992) and ATFa (Wicks lab, unpublished results). Thus, I tested PKA to see if it could phosphorylate ATF2 and/or ATFa. PKA was incubated alone, with histone f_2b (positive control), and with ATF2 or ATFa. Figure 11 shows that both ATF proteins are phosphorylated by PKA. Note also the 53 kDa phosphorylated breakdown band in the ATF2-containing lane (lane 3).

From the results thus far, we can conclude that both ATF2 and ATFa are phosphorylated by GST-JNK_1 and PKA. In fact, judging from the intensity of the bands seen in the autoradiogram (Figure 11A) as compared to the intensity of the bands in the stained polyacrylamide gel (Figure 11B), it appears as though ATFa is a much better

substrate for PKA than ATF2. To our knowledge, this phosphorylation of ATFa by PKA has not been reported previously in the literature.

GST-p38 phosphorylation of ATF2.

The kinase known simply as p38 has been reported to phosphorylate ATF2 on the same residues as does JNK (Raingeaud, 1995). I conducted experiments with p38 similar to those done with ATF2 and GST-JNK_1. GST-p38 was expressed and purified in a fashion identical to that used to isolate GST-JNK_1. A 30 minute phosphorylation time course was performed with purified GST-p38 (250 ng) and ATF2 (400 ng). Figure 12 shows the results of this assay. As a positive control, GST-p38 was incubated with 20 μg myelin basic protein (MBP), a known substrate for this kinase. It is clear that MBP is heavily phosphorylated, indicating an active p38 preparation. It is also apparent, despite the autophosphorylation band, that ATF2 is phosphorylated by GST-p38. By comparing the autoradiogram (Figure 12A) with the stained gel (Figure 12B), it can readily be seen that the upper band in both figures is ATF2, while the lower band is GST-p38. It seems as though maximal phosphorylation of ATF2 occurs within 15 minutes, but this may be misleading. Figure 12B, lane 5, shows a more intensely stained p38 band in the polyacrylamide gel, indicating a higher concentration of GST-p38 in that one lane. This increase in the amount of kinase may explain the more intense band in the autoradiogram (Figure 12A, lane 5). Other than lane 5, the intensity of the GST-p38 phosphorylated ATF2 bands increases linearly as incubation time increases (data not shown). Thus GST-p38 phosphorylates ATF2 within 30 minutes.

The amounts of GST-p38 and ATF2 were varied as was done with GST-JNK_1 and ATF2. Figure 13 shows GST-p38 (500 ng) incubated with increasing amounts of ATF2 (100-800 ng) for 30 minutes in lanes 2-5. ATF2 (400 ng) was titrated with increasing amounts of GST-p38 (250 ng to 2 μg) in lanes 6-9. By the use of densitometry, relative levels of phosphorylation of GST-p38 and ATF2 could be determined. Figure 14 shows that the intensity of the ATF2 phosphorylated band increases with increasing amounts of ATF2. Figure 15 shows that as the GST-p38 amounts rise, the level of ATF2 phosphorylation also increases proportionately. The bands in Figure 13A directly correlate with those seen in Figure 13B (~76 kDa for ATF2, ~72 kDa for GST-p38). Thus ATF2 is a substrate for GST-p38 *in vitro*, and this phosphorylation occurs within 30 minutes, using as little as 500 ng of GST-p38.

Titration of ATF2 and ATFa against GST-p38.

ATF2 and ATFa have a high sequence homology, including the conserved threonine residues (69 and 71 in ATF2, 51 and 53 in ATFa) known to be the site of phosphorylation in ATF2 by both JNK and p38 (Livingstone et al., 1995, van Dam et al., 1995, and Raingeaud, 1995). Both are also phosphorylated by both PKA and JNK_1 (Figures 5, 6, 9,10, and 11). It was reasonable, therefore to expect that both ATF2 and ATFa might be phosphorylated to a similar degree by GST-p38. As a test of this possibility, a titration of ATF2 and ATFa with a set concentration of GST-p38 (250 ng) was performed. As shown in Figure 16, the results with ATFa were surprisingly different than those with ATF2. ATF2 is readily phosphorylated by GST-p38. In marked contrast,

even the highest amount of ATFa tested was not phosphorylated by GST-p38. Figure 16B shows that GST-p38 migrates at a position between ATF2 and ATFa. The ATF2 band migrates at ~75 kDa, the ATFa band at ~69 kDa, while GST-p38 has a mobility directly between the two at ~72 kDa. The ATFa band is easily seen in the stained gel, but not at all in the autoradiogram taken from that same gel (Figure 16A). Figure 17 shows that as the amount of ATF2 increases, so does the level of the ATF2 breakdown product. The differences seen between Figure 17 and Figure 14 are due to the fact that the GST-p38 preparation used had aged, decreasing specific activity and increasing autophosphorylation. Densitometry was unable to detect any phosphorylation of ATFa. This represents a surprising new discovery; ATFa appears not to be a substrate for GST-p38 *in vitro*.

GST-p38/ATFa time course

As an additional check on the observed difference in the ability of GST-p38 to phosphorylate ATF2 and ATFa, a time course was performed with GST-p38 and ATFa. Five hundred ng of GST-p38 was incubated with approximately 300 ng of ATFa for up to 30 minutes. As is seen in Figure 18, at no time point was any phosphorylation of ATFa by GST-p38 detectable. The ATFa band is clearly seen in Figure 18B, but no phosphorylated band at the same molecular weight (~69 kDa) appears in Figure 18A. Superimposing the autoradiogram over the polyacrylamide gel, it becomes obvious that the band seen corresponds to GST-p38 autophosphorylation. Again, ATFa is not phosphorylated by GST-p38.

Titration of GST-p38 and ATFa

In yet another attempt to detect phosphorylation of ATFa by GST-p38, increasing amounts of GST-p38 (up to 2500 ng) were incubated with 300 ng of ATFa. Figure 19 shows that no phosphorylation of ATFa is detected with any amount of GST-p38, despite the obvious increase in GST-p38 autophosphorylation. Figure 20 shows that the level of GST-p38 autophosphorylation rises linearly with increasing concentrations of GST-p38. This increase in autophosphorylation was seen with every other GST-p38 titration performed (data not shown), and autophosphorylation of p38 has been reported in many papers (Kumar et al., 1997).

Conclusions

We conclude that ATFa is either not a substrate of p38 *in vitro* or, at the very least, it is a very poor one relative to ATF2. In support of this finding, Li and Wicks have found that overexpression of a constitutively active form of MKK6 (a potent activator of the p38 kinase cascade) in CHO cells did not result in further activation by ATFa of a CAT reporter with a partial CRE in its promoter but did further enhance the effects of ATF2 on CAT activity. The effects of both ATF2 and ATFa on CAT activity were enhanced when overexpressed with a constitutively active form of MKK7, an activator of the JNK pathway. This fits with the findings that both ATF2 and ATFa can be phosphorylated by GST-JNK_1 *in vitro*.

Both ATF2 and ATFa have been found to be the targets of the adenovirus E1a protein *in vivo* (Liu and Green, 1990, and Chatton et al., 1993). Much attention has been

devoted to the study of ATF2. Less notice has been paid to ATFa, however. Because phosphorylation has been shown to be a prerequisite for transcriptional activation of ATF2 (van Dam et al., 1995, Gupta et al., 1995, and Livingstone et al., 1995), we decided to compare the ability of various kinases known to phosphorylate ATF2 to phosphorylate ATFa.

Phosphorylation of transcription factors has been implicated in both activation and inhibition of transcriptional activity. Phosphorylation of sites in the DNA binding region of a transcription factor would place a strong negative charge in proximity to the negatively charged DNA backbone, preventing DNA binding by the transcription factor. Such an example is seen with phosphorylation of Sp1 by casein kinase II (CKII)) (Armstrong et al, 1997). CKII has also been shown to negatively regulate c-Jun binding to DNA through phosphorylation (Lin et al., 1992). PKA and PKC phosphorylation in the DNA binding region of the transcription factor LAP has been shown to prevent DNA binding (Trautwein et al., 1994). Thus phosphorylation may play a role in negatively influencing the action of transcription factors by preventing DNA binding. Phosphorylation may simply cause a conformational change, disrupting the proposed N terminal-C terminal intramolecular interactions. While phosphorylation of ATF2 by the MAP kinases ERK1 and ERK2 have been suggested to increase binding of bacterially expressed ATF2 to DNA *in vitro*, other labs have not achieved the same results (Abdel-Hafiz et al., 1992, Gong et al., 1995).

Members of the bZip family of transcription factors only bind DNA in homo- or heterodimer forms (Meyer and Habener, 1993). Phosphorylation may play a role in

influencing dimer formation, or perhaps partner selection. Both ATF2 and ATFa display intramolecular interactions between the N-terminal (the zinc finger containing) and C-terminal (bZip containing) domains (Li and Green, 1996 and Bocco et al., 1995). Such interaction prevents dimer formation, and subsequently DNA binding. Phosphorylation may disrupt this interaction, enabling successful dimer formation. ATFa0, a variant of ATFa missing 173 amino acids, forms a dominant negative heterodimer with ATFa. A similar variant of ATF2 has been identified, mXBP2 (Pescini et al., 1994). Phosphorylation of one or both halves of this dimer might disrupt this interaction, allowing dimerization with a partner that would enable DNA binding.

The most widely reported effect of phosphorylation of transcription factors is direct activation of transcription. Phosphorylation of CREB on serine 133 by PKA has been shown to be a requirement for transactivation ability (Bodor et al., 1995). ATF2 phosphorylation at threonines 69 and 71 by p38 and JNK leads to activation in a number of systems (Gupta et al., 1995, Livingstone et al., 1995, van Dam et al., 1995), and the N-terminal domain is also responsible for E1a mediated activation (Liu and Green, 1990, Livingstone et al., 1995). One possible mechanism for this activation is that phosphorylation of Thr 69 and Thr 71 enables protein-protein interactions either directly with constituents of the basal transcription machinery, or with a bridging protein such as CBP or p300. CBP/p300 binding may substitute for the E1a interaction seen in viral systems. CBP has been shown to interact with PKA phosphorylated CREB (Bodor et al., 1995). The JNK phosphorylation sites in cJun, Ser 63 and Ser 73, analogous to Thr 69 and Thr 71 in ATF2, have been shown to be crucial for the binding of that transcription

factor to CBP (Bannister et al., 1995), but phosphorylation of Ser 63 and 73 was not a prerequisite. Thus it is possible that phosphorylation of ATF2 at Thr 69 and Thr 71 leads to activation of transcription by enabling protein-protein interactions between the transcription factor and a protein such as CBP or p300 that itself directly contacts and thereby recruits transcription machinery. Because ATFa, like ATF2, is phosphorylated by members of the JNK family, and the sites of phosphorylation in ATF2 are highly conserved in ATFa (Thr 51 and Thr 53 in ATFa), it is possible that phosphorylation of ATFa can also lead to CBP/p300 interactions.

p38, as well as JNK, phosphorylates ATF2 on Thr 69 and 71 (Raingeaud, 1995), and this region is highly conserved in ATFa. Thus it is interesting that p38 does not phosphorylate ATFa. Perhaps the reason is that ATFa requires phosphorylation by a different kinase on a different site, causing a conformational change allowing p38 to bind and phosphorylate ATFa. Perhaps the binding site for p38 in ATF2 requires a three-dimensional conformation that is different or absent in ATFa. Isoforms of p38, p38-2 and p38γ, are expressed predominantly in skeletal muscle. p38-2 has been reported to be over 100 times more catalytically active than p38 in phosphorylating ATF2, but p38γ did not phosphorylate ATF2 at all (Stein et al., 1997 and Kumar et al., 1997). It would be interesting to see if ATFa is a substrate for any of these alternate forms of p38, perhaps implying a cell type specific role for the transcription factor.

The other major difference reported between ATFa and ATF2 is the differing effect of activation of a TGF-β2 promoter-driven CAT construct in the presence of pRb in CHO cells (Gong et al., 1995). Coexpression of pRb with ATF2 results in enhanced

activation, while coexpression of pRb with ATFa greatly reduced activation of the CAT reporter. Since pRb and TGF-β2 are both implicated in the regulation of cell cycle progression, these differences become even more intriguing. Opposing effects of the ERK pathway and the JNK/p38 pathway in regulating apoptosis have been reported (Xia et al., 1995). This may imply that ATFa and ATF2 play a major role in cell cycle checkpoint decisions, with the differences in phosphorylation by p38 playing a part in the signaling of this effect.

Chapter 4

Future Studies

1) Affinity pull-down of GST-tagged kinase or His-tagged substrates.

In order to overcome the difficulties of autophosphorylation by the kinases being studied, either kinase or substrate can be isolated from the kinase assay through GST-agarose or nickel-sepharose. My attempts at using this technique have met with varying degrees of success thus far.

2) Pre-phosphorylation of ATFa with PKA or JNK_1 before p38

Phosphorylating ATFa with either PKA or JNK_1 and non-radioactive ATP may make ATFa a substrate for p38. Prephosphorylation may cause a conformational change that overcomes negative regulation (e.g. N-C terminal interactions etc.) allowing p38 better access to potential phospho-acceptor sites.

3) Phosphorylation of ATFs by other kinases

Kinases such as CKII, p38-2, and p38γ may target ATFa or ATF2 *in vitro* and this phosphorylation may provide evidence for which kinase cascades influence the function of ATFa and ATF2.

4) Gel shift assays

The effects of phosphorylation on the ability of ATFa and ATF2 to bind DNA can be studied through gel shift assays. Phosphorylation by JNK, p38 or any of its isoforms,

CKII, or PKA with non-radioactive ATP may modify the ability of ATFa or ATF2 to bind a radioactive CRE-containing oligo.

5) 2-D phosphopeptide mapping

The regions of phosphorylation of ATFa and ATF2 can be determined through 2-D phosphopeptide mapping and the maps of ATF2 and ATFa can be compared to see if the pattern of phosphorylation is similar between the two proteins.

6) Heterodimerization

Finally, the effect of phosphorylation on the formation of heterodimers between the ATF proteins and other transcription factors such as cJun, cFos and others can be examined. Gel-shift assays before and after phosphorylation can be used to determine the effect of dimerization on the ability of ATFa or ATF2 to bind to varying olgionucleotides.

List of References

Abdel-Hafiz, H. A., Heasley, L. E., Kyriakis, J. M., Avruch, J., Kroll, D. J., Johnson, G. L., and Hoeffler, J. P., *Activating transcription factor-2 DNA-binding activity is stimulated by phosphorylation catalyzed by p42 and p54 microtubule-associated protein kinases.* Mol. Endocrinol., 1992. **6**, p2079-2089.

Armstrong, S. A., Barry, D. A., Leggett, R. W., and Mueller, C. R., *Casein kinase II-mediated phosphorylation of the C terminus of Sp1 decreases its DNA binding activity.* J. Biol. Chem., 1997. **272**, p13489-13495.

Bannister, A. J., Oehler, T., Wilhelm, D., Angel, P., and Kouzarides, T., *Stimulation of c-Jun activity by CBP: c-Jun residues Ser63/73 are required for CBP induced stimulation in vivo and CBP binding in vitro.* Oncogene, 1995. **11**, p2509-2514.

Bocco, J.L., Bahr, A., Goetz, J., Hauss, C., Kallunki, T., Kedinger, C., and Chatton, B., 1995. *In vivo association of ATFa with JNK/SAP kinase activities.* Oncogene, 1996. **12**, p1971-1980.

Bodor, J., Walker, W., Flemington, E., Spetz, A., and Habener, J. F., *Modulation of Tax and PKA-mediated expression of HTLV-I promoter via cAMP response element binding and modulator proteins CREB and CREM.* FEBS Letters, 1995. **377**, p413-418.

Chatton, B., Bocco, J. L., Gaire, M., Hauss, C., Reimund, B., Goetz, J., and Kedinger, C., 1993. *Transcriptional activation by the adenovirus larger E1a product is mediated by members of the cellular transcription factor ATF family which can directly associate with E1a.* Mol. Cell. Biol., 1993. **13**, p561-570.

Chatton, B., Bocco, J. L., Goetz, J., Gaire, M., Lutz, Y., and Kedinger, C., *Jun and Fos heterodimerize with ATFa, a member of the ATF/CREB family and modulate its transcriptional activity.* Oncogene 1994. **9**, p375-385.

van Dam, H., Wilhelm, D., Herr, I., Steffen, A., Herrlich, P., and Angel, P., *ATF-2 is preferentially activated by stress-activated protein kinases to mediate c-jun induction in response to genotoxic agents.* EMBO J., 1995. **14**, p1798-1811.

Du, W., Thanos, D., and Maniatis, T., *Mechanisms os transcriptional synergism between distinct virus-inducible enhancer elements.* Cell, 1993. **74**, p887-898.

Gaire, M., Chatton, B., and Kedinger, C., *Isolation and characterization of two novel, closely related ATF cDNA clones from HeLa cells.* Nucleic Acids Res., 1990. **18**, p3467-3473.

Goetz, J., Chatton, B., Mateeei, M-G., and Kedinger, C., *Structure and expression of the ATFa gene.* J. Biol. Chem., 1996. **271**, 29589-29598.

Gong, Q. Q., Huang, Z., and Wicks, W., *Interaction of retinoblastoma gene product with transcription factors ATFa and ATF2.* Arch. Biochem. Biophys., 1995. **319**, p445-450.

Gupta, S., Campbell, D., Derijard, B., and Davis, R., *Transcription factor ATF2 regulation by the JNK signal transduction pathway.* Science, 1995. **267**, p389-392.

Hai, T., and Curran, T., *Cross-family dimerization of transcription factors Fos/Jun and ATF/CREB alters DNA binding specificity.* Proc. Natl. Acad. Sci. USA, 1991. **88**, p3720-3724.

Kaszubska, W., van Huijsduijnen, R., H., Ghersa, P., DeRaemy-Schenk, A., Chen, B. P. C., Hai, T., DeLamarter, J. F., and Whelan, J., *Cyclic AMP-independent ATF family members interact with NF-κB and function in the activation of the E-selectin promoter in response to cytokines.* Mol. Cell. Biol., 1993. **13**, p7180-7190.

Kim, S. J., Wagner, S., Liu, F., O'Reilly, M. A., Robbins, P. D., and Green, M. R., *Retinoblastoma gene product activates expression of the human TGF-β2 gene through transcription factor ATF-2.*, Nature, 1992. **358**, p331-358.

Kumar, S., McDonnell, P. C., Gum, R. J., Hand, A. T., Lee, J. C., and Young, P.R., *Novel homologues of CSBP/p38 MAP kinase: activation, substrate specificity and sensitivity to inhibition by pyridinyl imidazoles.* Biochem. Biophys. Res. Comm., 1997. **235**, p533-538.

Li, X. Y., and Green, M. R., *Intramolecular inhibition of activating transcription factor-2 function by its DNA-binding domain.* Genes Dev., 1996. **10**, p517-527.

Li, Z., Jiang, Y., Ulevitch, R. J., and Han, J., *The primary structure of p38γ: a new member of p38 group of MAP kinases.*, Biochem. Biophys. Res. Comm., 1996. **228**, p334-340.

Lin, A., Frost, J., Deng, T., Smeal, T., Al-Alawi, N., Kikkawa, U., Hunter, T., Brenner, D., and Karin, M., *Casein kinase II is a negative regulator of c-Jun DNA and AP-1 activity.* Cell, 1992. **70**, p777-789.

Liu, F., and Green, M., *A specific member of the ATF transcription factor family can mediate transcription activation by the adenovirus E1a protein.* Cell, 1990. **61**, p1217-1224.

Livingstone, C., Patel, G., and Jones, N., *ATF-2 contains a phosphorylation-dependent transcriptional activation domain.* EMBO J., 1995. **14**, p1785-1797.

Maekawa, T., Sakura, H., Kanei-Ishii, C., Sudo, T., Yoshimura, T., Fujisawa, J., Yoshida, M., and Ishii, S., *Leucine zipper structure of the protein CRE-BP1 binding to the cyclic AMP response element in brain.* EMBO J., 1989. **8**, p2023-2028.

Meyer, T. E., and Habener, J. F., *Cyclic adenosine 3', 5'-monophosphate response element binding protein (CREB) and related transcription-activating deoxyribonucleic acid-binding proteins.* Endocr. Rev. 1993. **14**, p269-290.

Pescini, R., Kaszubska, W., Whelan, J., DeLamarter, J. F., and van Huijsduijnen, R. H., *ATF-a0, a novel variant of the ATF/CREB transcription factor family, forms a dominant transcription inhibitor in ATF-a heterodimers.* J. Biol. Chem., 1994. **269**, p1159-1165.

Raingeaud, J., Gupta, S., Rogers, J. S., Dickens, M., Han, J., Ulevitch, R. J., and Davis, R. J., *Pro-inflammatory cytokines and environmental stress cause p38 mitogen-activated protein kinase activation by dual phosphorylation on tyrosine and threonine.* J. Biol. Chem., 1995. **270**, p7420-7426.

Raingeaud, J., Whitmarsh, A. J., Barrett, T., Derijard, B, and Davis, R. J., *MKK3- and MKK6-regulated gene expression is mediated by the p38 mitogen-activated protein kinase signal transduction pathway.* Mol. Cell. Biol., 1996. **16**, p1247-1255.

Read, M. A., Whitley, M. Z., Gupta, S, Pierce, J. W., Best, J., Davis, R. J., and Collins, T., *Tumor necrosis factor α-induced E-selectin expression is activated by the nuclear factor-κB and c-Jun N-terminal kinase/p38 mitogen-activated protein kinase pathways.* J. Biol. Chem., 1997. **272**, p2753-2761.

Reimold, A. M., Grusby, M. J., Kosaras, B., Fries, J. W. U., Mori, R., Maniwa, S., Clauss, I. M., Collins, T., Sidman, R. L., Glimcher, M. J., and Glimcher, L. H., *Chondrodysplasia and neurological abnormalities in ATF-2-deficient mice.* Nature, 1996. **379**, p262-265.

Stein, B., Yang, M. X., young, D. B., Janknecht, R., Hunter, T., Murray, B. W., and Barbosa, M. S., *p38-2, a novel mitogen-activated protein kinase with distinct properties.* J. Biol. Chem., 1997. **272**, p19509-19517.

Trautwin, C., van der Geer, P., Karin, M., Hunter, T., and Chojkier, M., *Protein kinase A and C site-specific phosphorylations of LAP (NF-IL6) modulates its binding affinity to DNA recognition elements.* J. Clinic. Inves., 1994. **93**, p2554-2561.

Xia, Z., Dickens, M., Raingeaud, J., Davis, R. J., and Greenberg, M. E., *Opposing effects of ERK and JNK-p38 MAP kinases on apoptosis.* Science, 1995. **270**, p1326-1331.

Appendix

Figure 1

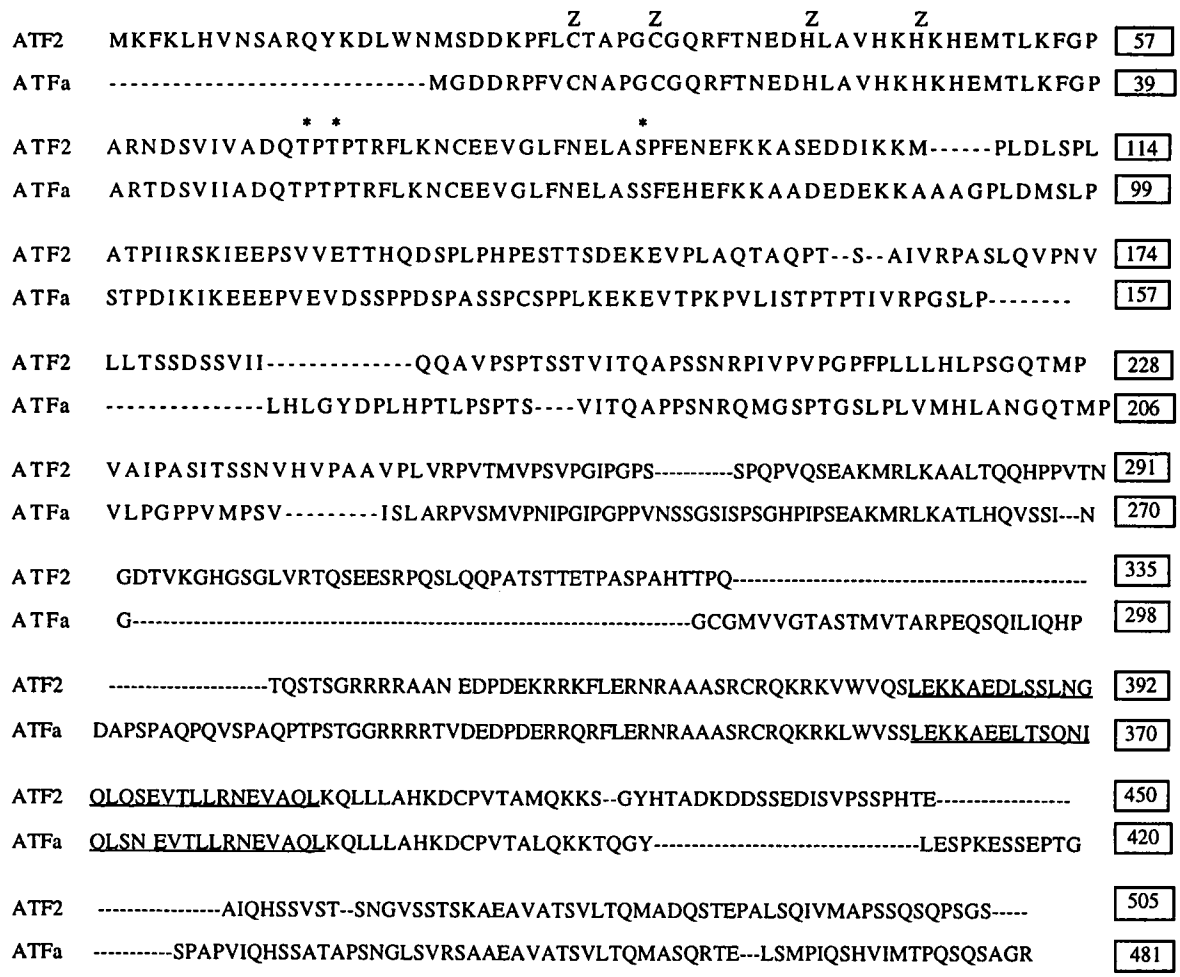


Figure 1: Sequence Comparison of ATF2 and ATFa.

The amino acid sequence of ATF2 and ATFa are aligned to show the many similarities. A "Z" indicates residues composing the zinc finger region. The asterisks indicate known sites of phosphorylation in ATF2. The underlined region of both proteins represents the leucine zipper domain. The numbers in boxes represent the position of the last amino acid shown in that line.

Figure 2

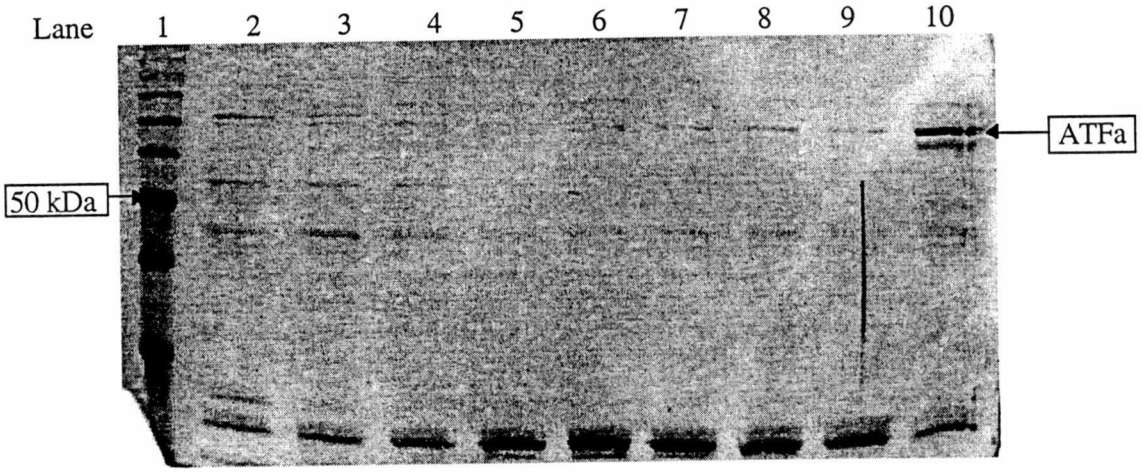


Figure 2: Nickel-Sepharose Affinity Column Purification of ATFa.

Bacteria transformed with pET vector containing the ATFa coding sequence were lysed and crude extracts were isolated. Two ml of this crude lysate were applied to a nickel-sepharose affinity column. The column was washed with an increasing gradient of imidazole ranging from 5 to 100 mM. ATFa was eluted by the addition of 200 mM imidazole. Fractions were loaded onto a 10% SDS-PAGE and silver stained to visualize bands. Lane 1 is a 10 kDa ladder molecular weight standard. Lanes 2-9 contain fractions 10-17 of the imidazole wash gradient, respectively, while lane 10 contains the 200 mM elution fraction. The identity of the bands seen in lane 10 were confirmed through Western blotting (data not shown).

Figure 3

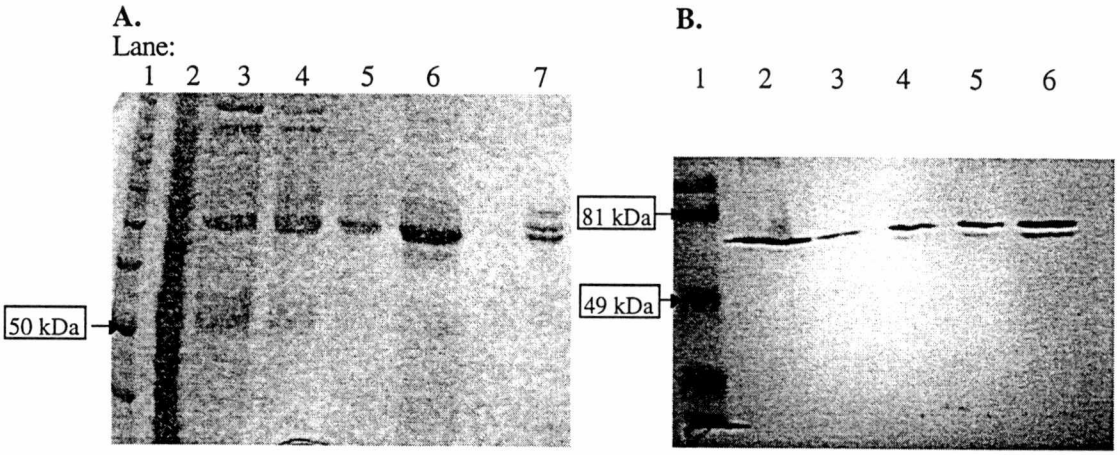


Figure 3: Affinity Column Purification of ATFa with Urea Gradient Wash.
Two ml of ATFa-containing crude cellular lysate were applied to a nickel-sepharose affinity column, as in Figure 2. The column was then washed with a decreasing gradient of urea ranging from 6 M to 0M. The column was then washed with 40 mM before eluting with 200 mM imidazole. **A)** Collected fractions were examined through a 10% polyacrylamide gel. Lane 1 contains a 10 kDa molecular weight standard. Lane 2 contains crude lysate, lanes 3 and 4 show 40 mM imidazole fractions while lanes 5 and 6 show 200 mM imidazole fractions respectively. Lane 7 contains the same sample of ATFa shown in Figure 2, lane 10. **B)** Western blotting was used to confirm the identity of the bands seen in Figure 3A. Lane 1 contains a prestained standard. Lanes 2-6 contain the same samples in the same amounts as in Figure 3A. The primary antibody used in this blot was mouse monoclonal anti-T7, specific for a peptide fragment encoded in the pET expression vector system.

Figure 4

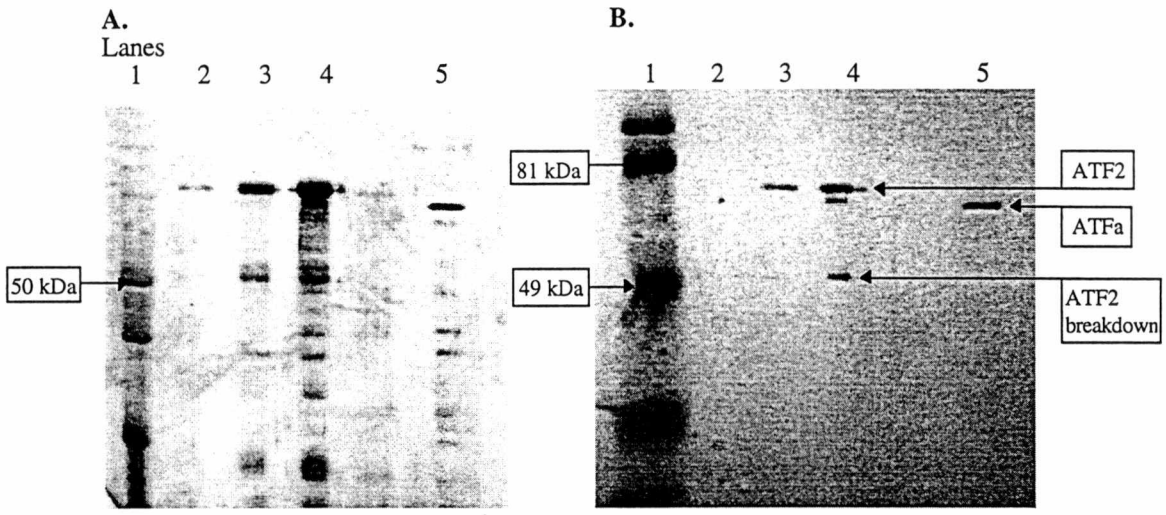


Figure 4: Comparison of Concentrations of Purified ATF2 and ATFa.

Three known concentrations of purified ATF2 (Santa Cruz) were compared with an unknown concentration of purified ATFa. **A)** This silver stained 10% polyacrylamide gel contained 200 ng, 400 ng and 800 ng of ATF2 in lanes 2-4 respectively. Lane1 contains a 10 kDa ladder molecular weight standard. Lane 5 contains 4µl of ATFa (200 mM fraction 2 from Figure 3A lane 6). The doublet seen with ATFa is present in this fraction, but it is very faint. **B)** Western blotting was used to confirm the identity of the ATF2 and ATFa bands. Lane 1 contains a prestained molecular weight standard. Lanes 2-5 contain the same fractions in the same concentrations as in **A)**. Notice the breakdown product at 50 kDa in lane 4. This band must be an amino-terminal peptide due to the fact it is detected by the anti-T7 antibody. Both of these proteins were purified from the same expression vector (pET 14b) in the same system (*E. coli)* . Proteolysis is a common problem in all of the samples, whether purchased or purified in the lab. The concentration of ATFa can be estimated to be between 200 and 400 ng in 4 µl, or about 75 ng/µl.

Figure 5

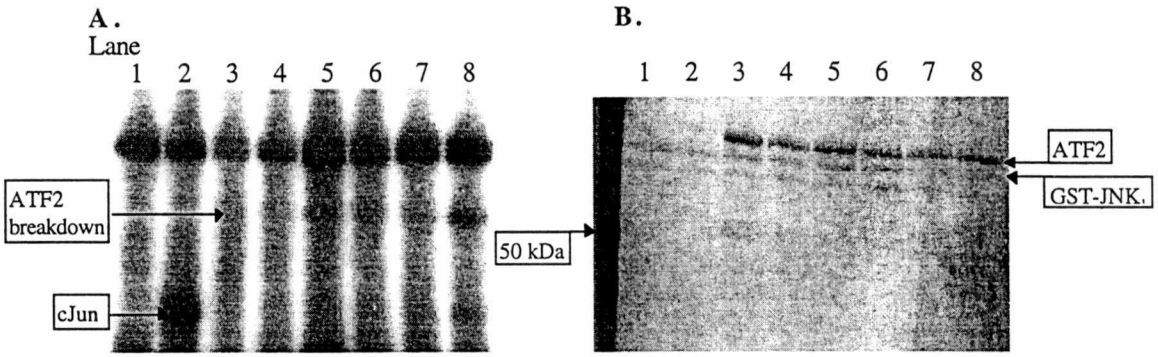


Figure 5: GST-JNK$_1$/ATF2 Phosphorylation Time Course.

A) Lane 1 shows GST-JNK$_1$ (50 ng) alone as a test for autophosphorylation. Lane 2 is a positive control, showing GST-JNK$_1$ phosphorylation of GST-cJun (1-79). Lanes 3-8 show kinase reactions with 50 ng of GST-JNK$_1$ and 400 ng of ATF2, with samples taken at five minute intervals. **B)** The stained gel used to produce the autoradiogram. The ATF2 breakdown product seen in figure 4 appears to contain a phosphorylation site for GST-JNK$_1$, since a faint band can be seen at the same molecular weight (~53 k Da).

Figure 6

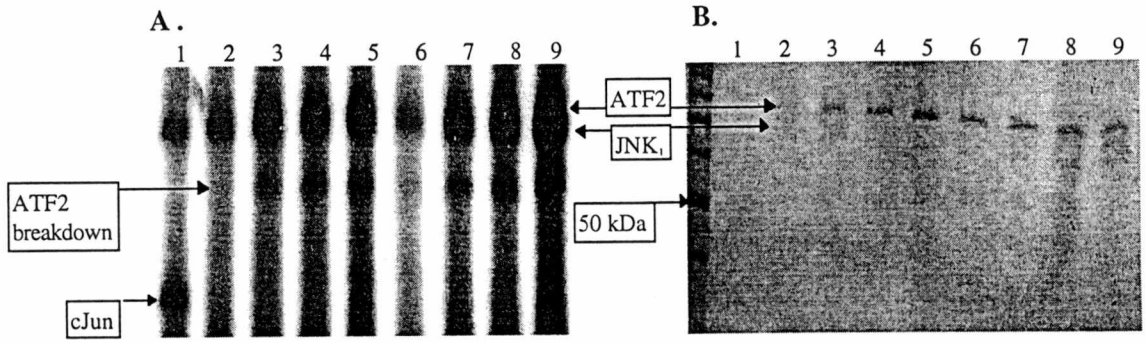


Figure 6: Titration of GST-JNK$_1$ and ATF2.

A) Lane 1 is a positive control, with GST-JNK$_1$ and GST-cJun (1-79). Lanes 2-5 contain increasing amounts of ATF2 (100 ng, 200 ng, 400 ng and 800 ng respectively) titrated against a set concentration of GST-JNK$_1$ (50 ng). Lanes 6-9 contain increasing amounts of GST-JNK$_1$ (25 ng, 50ng, 100 ng and 200 ng respectively) with a set amount of ATF2 (400 ng). **B)** The Comassie stained gel used to produce the autoradiogram is shown to give the relative positions of ATF2 and GST-JNK$_1$. Notice the phosphorylated breakdown product seen in the lanes with ATF2 (Santa Cruz). This band is at the same molecular weight (~53 kDa) as that seen in Figures 4 and 5.

Figure 7

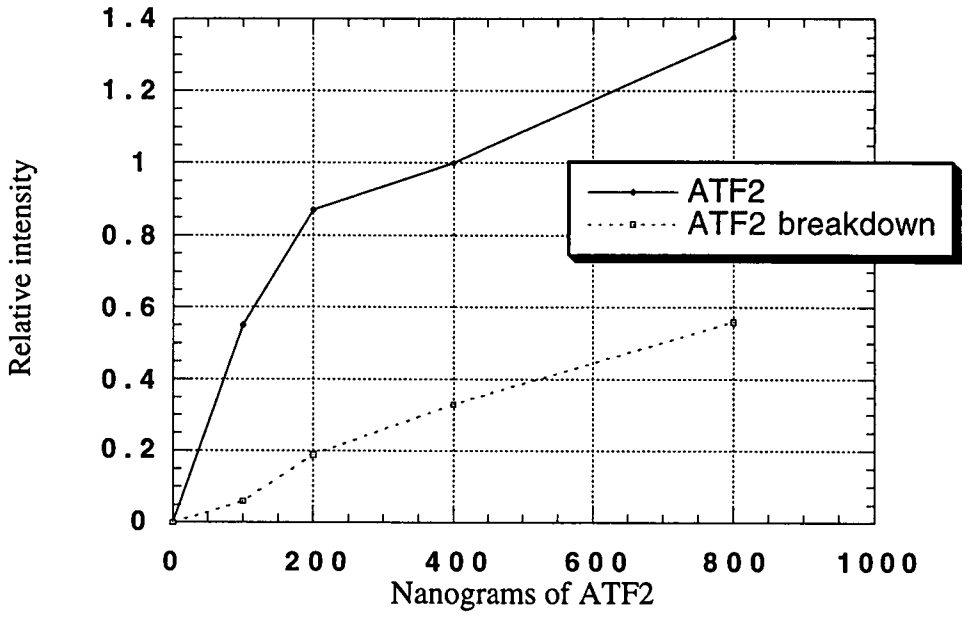


Figure 7: Densitometric Measurement of the Titration of ATF2 with GST-JNK$_1$.
This graph shows phosphorylation of increasing amounts of ATF2 and the ATF2 breakdown product by 50 ng of GST-JNK$_1$. The increase in phosphorylation is proportional between the two, despite the fact that the breakdown product is not as abundant as full length ATF2. In fact, it appears as if the breakdown product is a better substrate than full length ATF2. GST-JNK$_1$ autophosphorylation did not increase significantly with increasing amounts of ATF2.

Figure 8

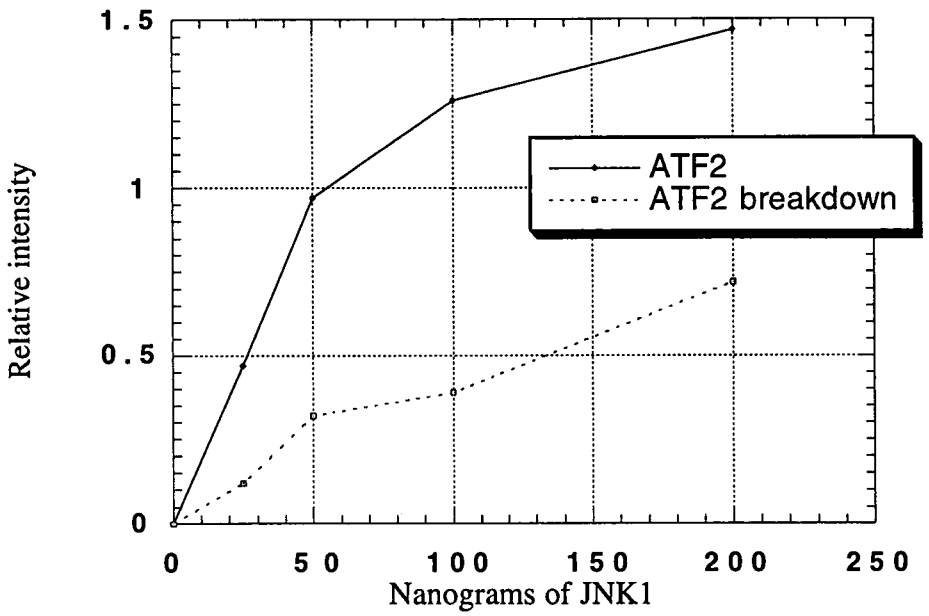


Figure 8: Densitometric Measurement of the Titration of GST-JNK$_1$ with ATF2.
This graph shows phosphorylation of 400 ng ATF2 and the ATF2 breakdown product by increasing amounts of GST-JNK$_1$. Both the full length and the ~53 kDa breakdown product are phosphorylated to a higher degree as the concentration of GST-JNK$_1$ increase. The level of GST-JNK$_1$ autophosphorylation increased linearly as the amount of kinase increased.

Figure 9

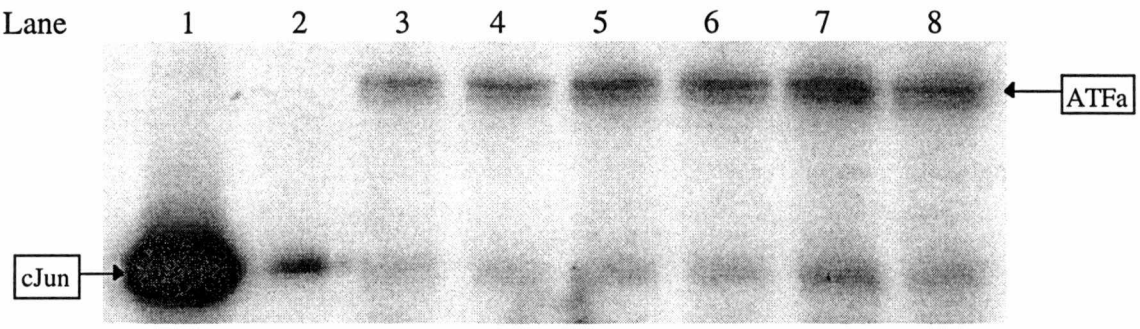


Figure 9: GST-JNK$_1$/ATFa Phosphorylation Time Course.
A GST-JNK$_1$ kinase assay was performed as described in Materials and Methods. GST-JNK$_1$ (50 ng) was incubated with approximately 300 ng of purified ATFa for up to 30 minutes at 30°. Lane 1 is a positive control, showing JNK$_1$ phosphorylation of GST-cJun (1-79). Lane 2 contains ATFa alone. Lanes 3-8 show reactions stopped at five minute intervals from 5 to 30 minutes respectively. The bands seen in this autoradiogram directly coincide with those seen on the stained gel at the position corresponding to ATFa, approximately 70 kDa.

Figure 10

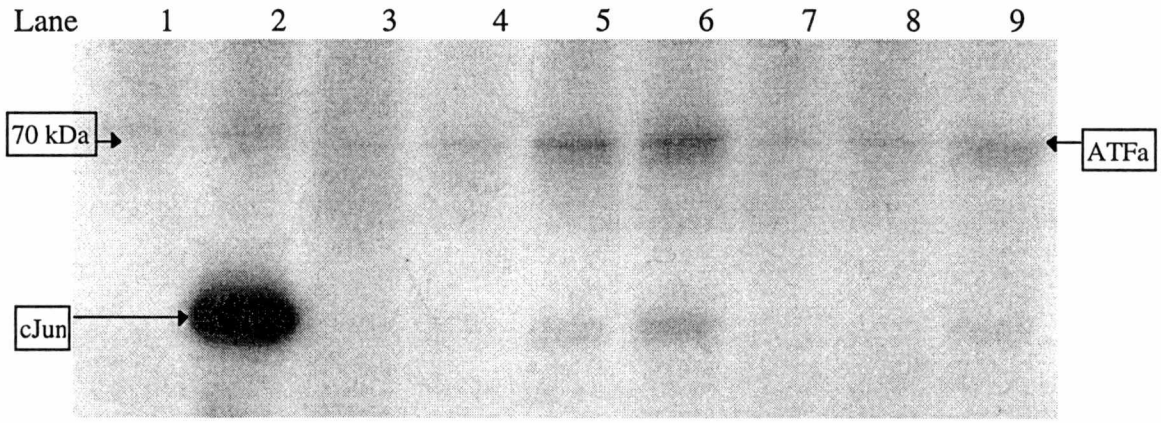


Figure 10: Titration of GST-JNK$_1$ and ATFa.
A GST-JNK$_1$ kinase assay was performed as described in Materials and Methods. All reactions were conducted for 30 minutes at 30°. Lane 1 contains GST-JNK$_1$ alone (50 ng). Lane 2 is a positive control for kinase activity, containing GST-JNK$_1$ and GST-cJun (1-79). Lane 3 is ATFa alone (no kinase) as a negative control. Lanes 4-6 show the result of adding increasing amounts of GST-JNK$_1$ (25 ng, 50 ng and 100 ng respectively) on the phosphorylation of a set amount of ATFa (300 ng). Lanes 7-9 show the result of adding increasing amounts of ATFa (150 ng, 300 ng, and 600 ng respectively) with a set amount of kinase (50 ng).

Figure 11

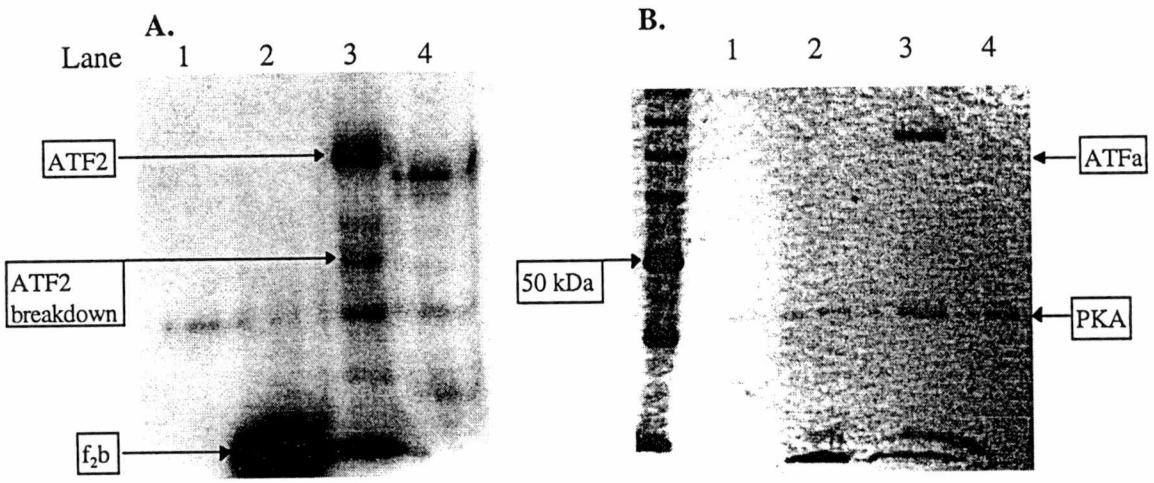


Figure 11: cAMP Dependent Kinase (PKA) Phosphorylation of ATF2 and ATFa.
A modified kinase assay (PKA kinase assay) was used as described in Materials and Methods. PKA (2.5 units/µl; Sigma) was incubated in PKA reaction buffer alone in lane 1. Lane 2 is a positive control, with 2.5 units of PKA with histone f_2b (2 µg). Lanes 3 and 4 show PKA (2.5 units) with ATF2 (800 ng) or ATFa (600 ng) respectively. **A)** Both ATF2 and ATFa are phosphorylated by PKA. **B)** The stained gel shows that not as much ATFa was loaded in lane 4 as compared to the amount of ATF2 loaded in lane 3. This was due to the fact that the wells in the gel could not hold the entire volume of the ATFa reaction, whereas all of the ATF2 reaction could fit in lane 3. Note again the phosphorylated ATF2 breakdown product as seen previously.

Figure 12

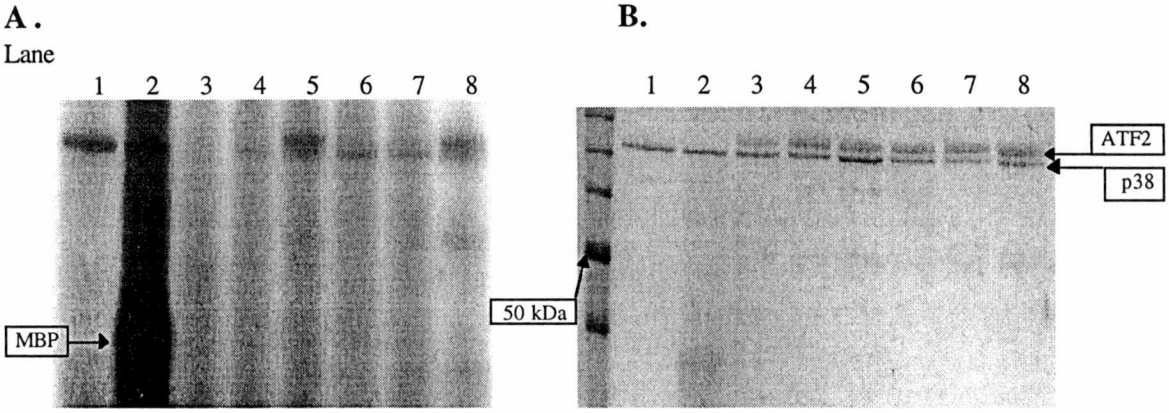


Figure 12: GST-p38/ATF2 Phosphorylation Time Course.
A) In this autoradiogram, Lane 1 shows GST-p38 alone (250 ng) as a test for autophosphorylation. Lane 2 is a positive control, with GST-p38 and myelin basic protein (MBP, 20 μg). Lanes 3-8 contain ATF2 (300 ng) and GST-p38 (250 ng) incubated together at 30° for up to 30 minutes. Samples were removed at five minute intervals. **B)** The stained gel used to form the autoradiogram shows the relative positions of GST-p38 and ATF2.

Figure 13

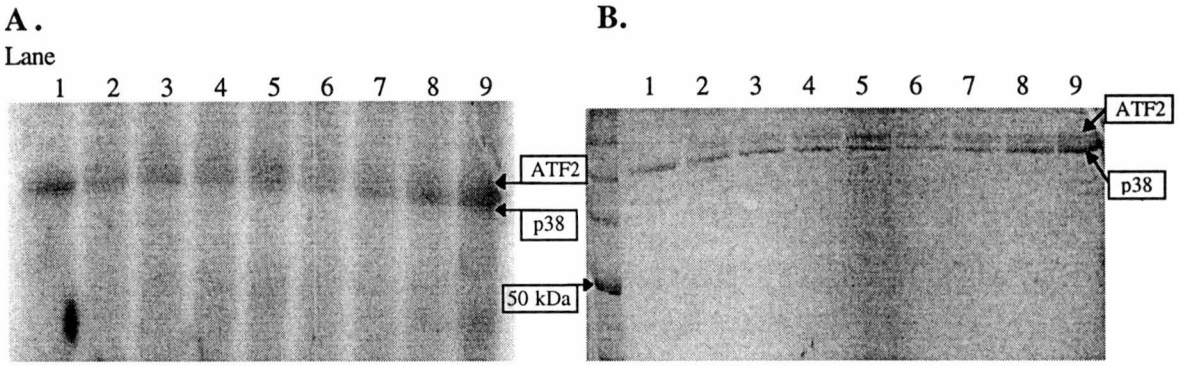


Figure13: Titration of GST-p38 and ATF2.

A) In this autoradiogram, Lane 1 contains 500 ng of GST-p38 alone as a test for autophosphorylation. Lanes 2-5 contain increasing amounts of ATF2 (100, 200, 400, and 800 ng respectively) incubated with a set concentration of GST-p38 (500 ng). Lanes 6-9 contain a set amount of ATF2 (400 ng) incubated with increasing amounts of GST-p38 (0.25, 0.5, 1.0, and 2.0 μg respectively). **B)** The Coomassie stained gel shows the relative position of ATF2 and GST-p38.

Figure 14

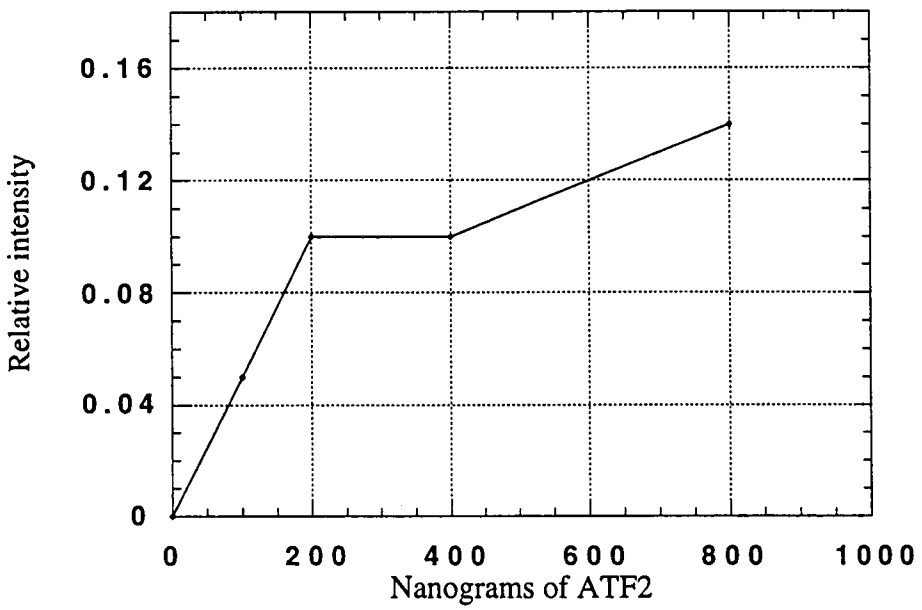


Figure 14: Densitometric Measurement of the Titration of GST-p38 with ATF2.
This graph shows phosphorylation of increasing amounts of ATF2 by 500 ng of GST-p38. GST-p38 autophosphorylation did not increase with increasing amounts of ATF2.

Figure 15

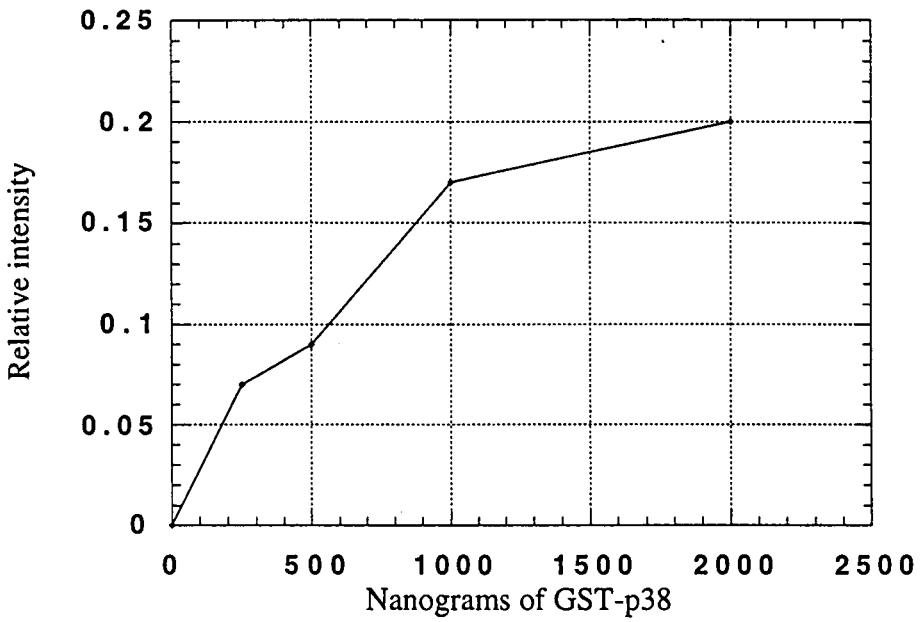


Figure 15: Densitometric Measurement of the Titration of ATF2 with GST-p38.
Increasing GST-p38 concentrations result in an increase in the degree of phosphorylation of 400 ng of ATF2. GST-p38 autphosphorylation levels increased linearly with increasing amount of kinase.

Figure 16

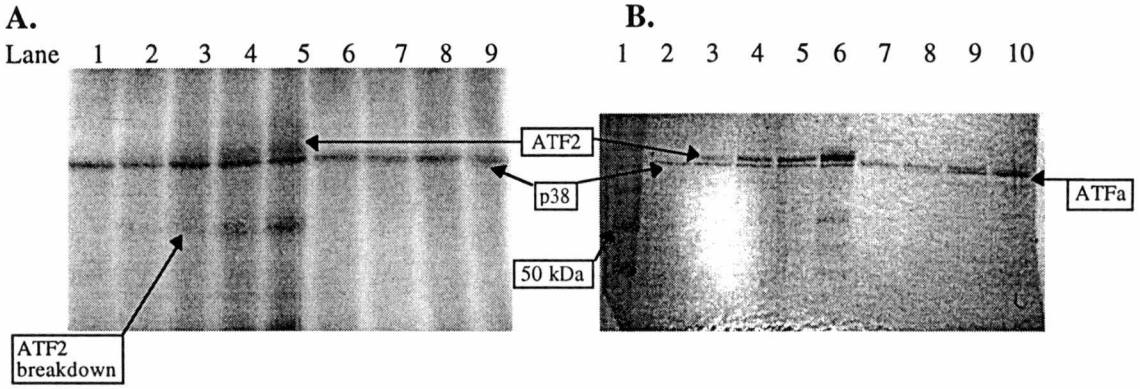


Figure 16: Titration of GST-p38 with ATF2 and ATFa.

A) A standard kinase assay was performed with GST-p38 and increasing amounts of either ATF2 or ATFa. Lane 1 is GST-p38 alone (250 ng). Lanes 2-5 contain GST-p38 (250 ng) and 100, 200, 400 or 800 ng of ATF2 respectively. Lanes 6-9 contain the same amount of GST-p38 with an increasing concentration of ATFa, 150, 300, 600 or 1200 ng. ATFa does not appear to be a good substrate for GST-p38. **B)** The Coomassie stained gel used to form the autoradiogram shows the relative positions of GST-p38, ATF2 and ATFa.

Figure 17

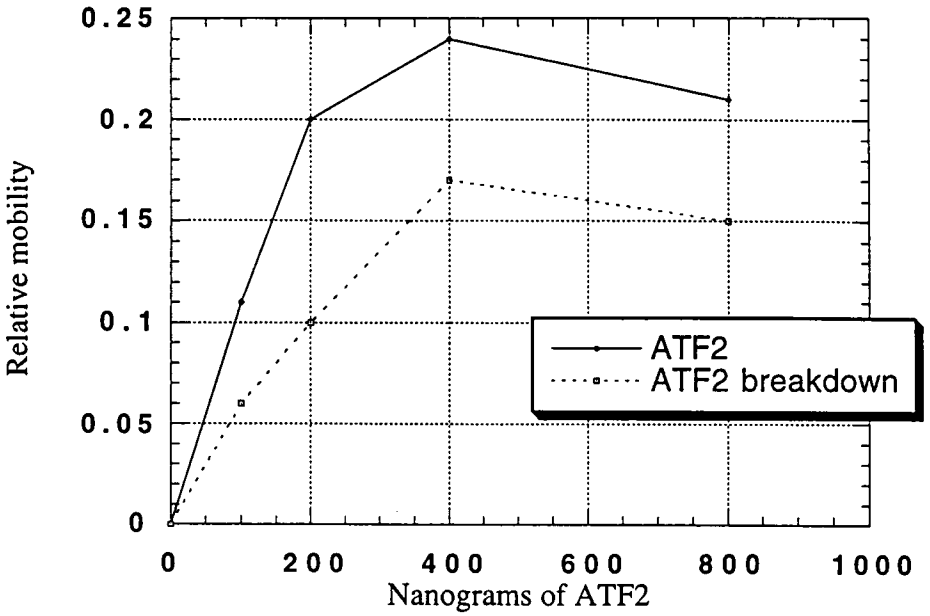


Figure 17: Densitometric Measurement of the Titration of ATF2 with GST-p38.
This graph shows the degree of phosphorylation of ATF2 and the ATF2 breakdown product by 250 ng of GST-p38. The degree of phosphorylation by GST-p38 between the two substrates follows the same pattern. GST-p38 autophosphorylation levels did not increase with increasing amounts of ATF2.

Figure 18

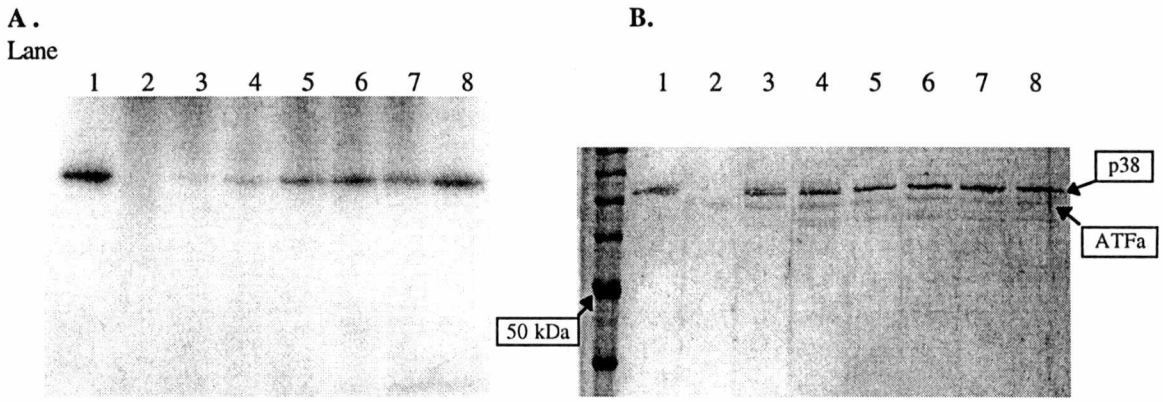


Figure 18: GST-p38/ATFa Phosphorylation Time Course.

A) A GST-p38 kinase assay was performed as described in Materials and Methods. GST-p38 (500 ng) was incubated alone in lane 1 as a test for autophosphorylation. Lane 2 contains ATFa alone as a negative control. Lanes 3-8 show GST-p38 (500 ng) with ATFa (300 ng) incubated together for intervals up to 30 minutes. Samples were removed every five minutes. **B)** The Coomassie stained gel used to form the autoradiogram shows the relative positions of GST-p38 and ATFa.

Figure 19

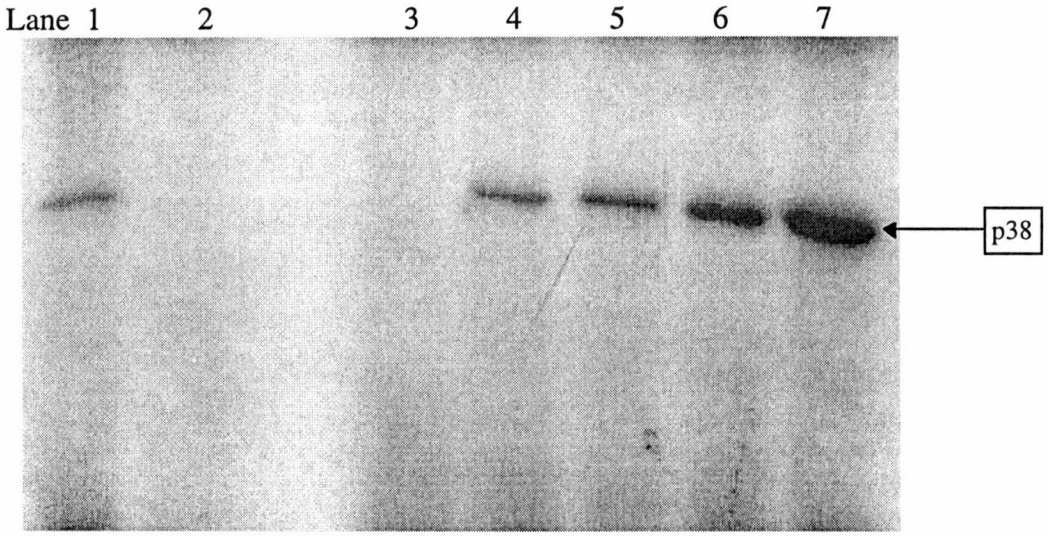


Figure 19: Titration of GST-p38 and ATFa.

Increasing amounts of GST-p38 were incubated in a GST-p38 kinase assay with a set concentration of ATFa. Lane 1 contains GST-p38 alone (500 ng) as a test for autophosphorylation. Lane 2 contains ATFa without GST-p38. Lanes 3-7 contain ATFa (300 ng) with increasing amounts of GST-p38 (0.125, 0.25, 0.5, 1.25, and 2.5 μg respectively). The downward slope apparent in lanes 4-7 is due to the gel not having been dried properly. It does not reflect the migration of bands seen on the Coomassie stained gel.

Figure 20

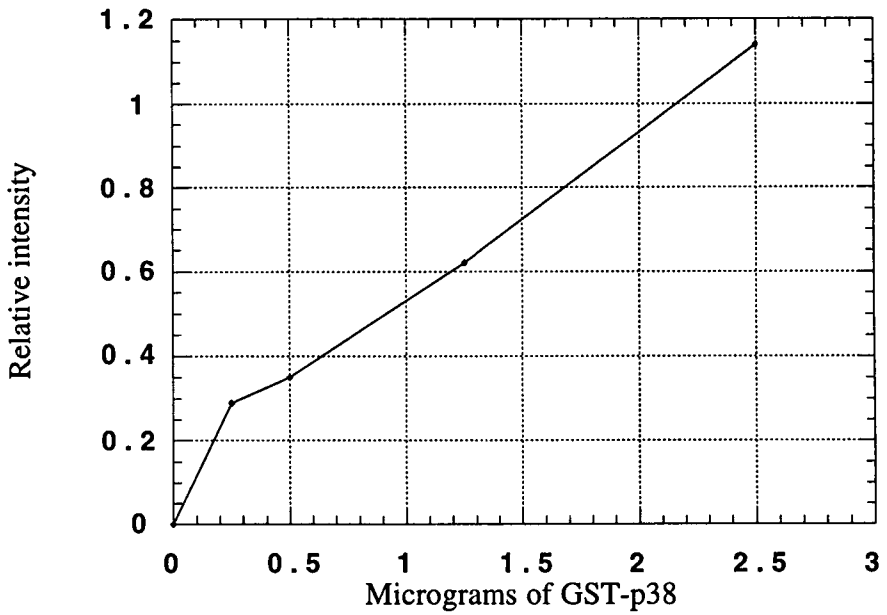


Figure 20: Densitometric Measurement of the Titration of GST-p38 with ATFa.
No phosphorylation of ATFa by GST-p38 was detectable by densitometry. GST-p38 autophosphorylation levels increased in a linear fashion.

VITA

John Blakemore was born in Dresden, Tennessee, on January 14, 1971. After graduation from Dresden High School in 1989, he enrolled in the University of Tennessee at Martin. He received a Bachelor of Science degree with a major in Biology in December of 1993.

He was admitted to the University of Tennessee, Knoxville in the Department of Biochemistry and Cellular and Molecular Biology in the fall of 1994. He was awarded the Master of Science degree in the Life Sciences: Biotechnology concentration in August of 1998.